AD_____

Award Number: W81XWH-06-1-0314

TITLE: Breast Cancer Lymphatic Dissemination-Influence of Estrogen and Progesterone

PRINCIPAL INVESTIGATOR: Joshua C. Harrell, Ph.D.
                                            Kathryn B. Horwitz, Ph.D.

CONTRACTING ORGANIZATION: University of Colorado Health Sciences Center
                                            Aurora, CO 80045-0508

REPORT DATE: October 2008

TYPE OF REPORT: Final

PREPARED FOR: U.S. Army Medical Research and Materiel Command
                      Fort Detrick, Maryland 21702-5012

DISTRIBUTION STATEMENT: Approved for Public Release;
                                      Distribution Unlimited

The views, opinions and/or findings contained in this report are those of the author(s) and should not be construed as an official Department of the Army position, policy or decision unless so designated by other documentation.

REPORT DOCUMENTATION PAGE

Form Approved
OMB No. 0704-0188

Public reporting burden for this collection of information is estimated to average 1 hour per response, including the time for reviewing instructions, searching existing data sources, gathering and maintaining the data needed, and completing and reviewing this collection of information. Send comments regarding this burden estimate or any other aspect of this collection of information, including suggestions for reducing this burden to Department of Defense, Washington Headquarters Services, Directorate for Information Operations and Reports (0704-0188), 1215 Jefferson Davis Highway, Suite 1204, Arlington, VA 22202-4302. Respondents should be aware that notwithstanding any other provision of law, no person shall be subject to any penalty for failing to comply with a collection of information if it does not display a currently valid OMB control number. **PLEASE DO NOT RETURN YOUR FORM TO THE ABOVE ADDRESS.**

1. REPORT DATE	2. REPORT TYPE	3. DATES COVERED
1 Oct 2008	Final	1 Mar 2006 – 28 Sep 2008

4. TITLE AND SUBTITLE

Breast Cancer Lymphatic Dissemination-Influence of Estrogen and Progesterone

5a. CONTRACT NUMBER

5b. GRANT NUMBER
W81XWH-06-1-0314

5c. PROGRAM ELEMENT NUMBER

6. AUTHOR(S)

Joshua C. Harrell, Ph.D.
Kathryn B. Horwitz, Ph.D.

E-Mail: oshua.harrell@uchsc.edu

5d. PROJECT NUMBER

5e. TASK NUMBER

5f. WORK UNIT NUMBER

7. PERFORMING ORGANIZATION NAME(S) AND ADDRESS(ES)

University of Colorado Health Sciences Center
Aurora, CO 80045-0508

8. PERFORMING ORGANIZATION REPORT NUMBER

9. SPONSORING / MONITORING AGENCY NAME(S) AND ADDRESS(ES)
U.S. Army Medical Research and Materiel Command
Fort Detrick, Maryland 21702-5012

10. SPONSOR/MONITOR'S ACRONYM(S)

11. SPONSOR/MONITOR'S REPORT NUMBER(S)

12. DISTRIBUTION / AVAILABILITY STATEMENT
Approved for Public Release; Distribution Unlimited

13. SUPPLEMENTARY NOTES

14. ABSTRACT Breast cancers commonly spread to lymph nodes (LNs). If the primary tumors are estrogen receptor (ER) and/or progesterone receptor (PR) positive, then the likelihood that LN metastases express receptors exceeds 80%. We developed metastasis models using ZsGreen labeled MCF-7 and T47D human breast cancer cells. Tumors were tracked in living mice by whole-body imaging, and macrometastases or micrometastases were detected by intravital imaging or fluorescence microscopy. Tumor growth was estrogen dependent and progesterone had minimal impact on tumor growth or metastasis. To determine if the LN microenvironment alters estrogen-dependent gene expression, we developed a unique model to identify estradiol regulated genes in ER+ breast tumors and LN metastases. Fluorescent ER+ MCF-7 tumors were grown in ovariectomized nude mice supplemented with estradiol. Once axillary LN metastasis arose, estradiol was withdrawn (EWD), for 1 or 4 weeks, or continued, to assess estradiol responsiveness. On EWD, proliferation rates fell similarly in tumors and LN metastases. However, estradiol-dependent ER down-regulation and PR induction were deficient in LN metastases, indicating that ER transcriptional activity was altered in the LN. Cancer cells from estradiol treated and EWD primary tumors and matched LN metastases were isolated by laser capture microdissection. Global gene expression profiling identified transcripts that were regulated by the tissue microenvironment, by hormones, or by both.. We propose that the LN microenvironment alters estradiol signaling and contributes to antiestrogen resistance.

15. SUBJECT TERMS
ER, PR, lymph node, metastasis, fluorescent proteins

16. SECURITY CLASSIFICATION OF:			17. LIMITATION OF ABSTRACT	18. NUMBER OF PAGES	19a. NAME OF RESPONSIBLE PERSON USAMRMC
a. REPORT	b. ABSTRACT	c. THIS PAGE			
U	U	U	UU	38	19b. TELEPHONE NUMBER *(include area code)*

Table of Contents

Introduction

Breast cancer spread into the lymph nodes (LN) is the single most deadly prognostic factor identified to date. Understanding factors that regulate cancer-cell colonization of the lymphatics is essential to prevent malignant invasion. Most breast cancers are estrogen (ER) and/or progesterone receptor (PR) positive, and the majority of breast cancers that spread to the LN maintain ER and PR expression. However, due to lack of experimental models of ER+ breast cancer metastasis, little is known about the roles of hormones in breast cancer spread to, and growth in, LNs.

Hypotheses: I postulated that breast cancer metastasis to LNs is dependent on tumor growth and tumor size. Second, I predicted that tumor spread to LNs is dependent on tumor associated lymphangiogenesis. Finally, I hypothesized that ER expression and transcriptional function is maintained in tumors and LN metastases.

Project goals: I planned to develop and then define models of ER+ breast cancer metastasis, in preparation for studies of hormone action that addressed hormonal regulation of key genes involved in lymphatic development, LN spread, and growth of cancer cells within the LNs.

Approved STATEMENT OF WORK:

Task 1. Develop and characterize all cell lines used in the study (Months 1-6).
   - **A. Make ZsGreen and DsRed-Express polyclonal stable cell lines.**
   - **B. Quantitation of ER and PR protein expression in each lines.**

Task 2. Assess the impact of systemic estrogen and progesterone on ER+/-PR+/- breast cancer lymphatic spread (Months 6-36).
   - **A. Grow and determine the rate of lymphatic invasion using homogeneous or dual colored mixed ER+/-, PR+/- tumors with no systemic hormones, E, P, E+P.**
   - **B. Perform immunohistochemistry on tumors, lymphatics, and LNs to understand effects of E and P on cancer cells, lymphatics, and LNs.**

**Task 3. Determine hormonal influence to tumor lymphangiogenesis (Months 8-36).**
   - **A. Determine hormone influence on gene expression of lymphangiogenic factors.**
   - **B. Immunohistochemically quantitate lymph vessels in each tumor line and determine the influence of hormones on lymphatic vessel development.**

Body

Task 1. The majority of the work for this task is summarized in my 2nd and 3rd first-author publications enclosed within the appendix (1-2) and within the year 2 annual report. In these papers and the previous report, I described the studies that complete and expand on task 1 of the approved statement of work. This includes; (a) using fluorescently labeled ER+ breast cancer cells (MCF-7 and T47D) to immunohistochemically quantify the amounts of ER and PR expression in the breast cancer cells grown *in vivo* (Harrell et al, CanRes 2007 Figure 2). This work expands on my 2006 first author publication (Harrell et al, CanRes 2006, figure 6). By using estradiol withdrawal post LN metastasis I was able to define the genes that are estrogen regulated in primary breast tumors compared to their LN metastases (Harrell et al, CanRes 2007 Figure 3. We confirmed that ER were highly expressed in mammary gland tumors of all estradiol-free mice, and they behaved normally, with ligand dependent downregulation upon estradiol treatment coupled to PR upregulation. However, these expression patterns were altered in metastases within the lymphatic vessels or in LNs, with poor ER downregulation and decreased PR induction. Thus, the lymphatic environment makes ER+ cancer cells estrogen insensitive. To study this further, I gene expression profiled estrogen-treated and estrogen-withdrawn tumors and matched LN metastases. For my first study (1) the microarray analysis was performed on laser-captured MCF-7 cells from tumors and LN metastases, instead of on whole-tissue. Interestingly, the array data confirmed the immunohistochemistry in that fewer genes were E regulated in LNs as compared to primary tumors (Harrell et al, CanRes 2007 Figure 6). Furthermore, some genes that were regulated in one direction by estradiol in the primary tumor were regulated in the opposite direction by estradiol in the LN metastasis (Harrell et al, CanRes 2007 Figure 6. These findings are very important as they provide further evidence that the LN microenvironment promotes estrogen resistance. My second study from this 2nd year of funding contrasted how whole-tissue versus laser-captured material alters LN metastasis gene signatures (2). Interestingly, I found that mouse RNA, which contaminates whole-organ microarray analyses, impacts the final data. The mouse hybridizes to and/or dilutes out the human RNA, on the human specific chips (Harrell et al, ClinExpMet Figure 2). I found that whole-tissue and laser-captured isolated RNA yield totally distinct "metastasis signatures" (Harrell et al, ClinExpMet Figure 3) and I speculate that the laser-capture-derived data are more accurate. **These studies complete task 1.**

Task 2. The majority of the work to complete task 2 was completed during the final year of the funding period. I performed studies that investigated how progesterone (or medroxy-progesterone acetate (MPA)) alone or in combination with estradiol affect ER+ tumor growth and metastasis. The findings of reduced PR expression (from task 1 above) in metastases suggested that treating mice with estradiol + progesterone may not affect cancer cells any differently once they become metastatic—as the amount of PR that can bind progesterone is diminished. Though progestin treatment led to a decrease in the percent of tumors that generated LN metastases, it is obvious that in this model system, if a

ER+ tumor grows to a certain size it will metastasize to the local or distal LNs (Figure 1). Further analyses of how progestin dose and duration of treatment effect metastases is warranted. **These studies complete task 2.**
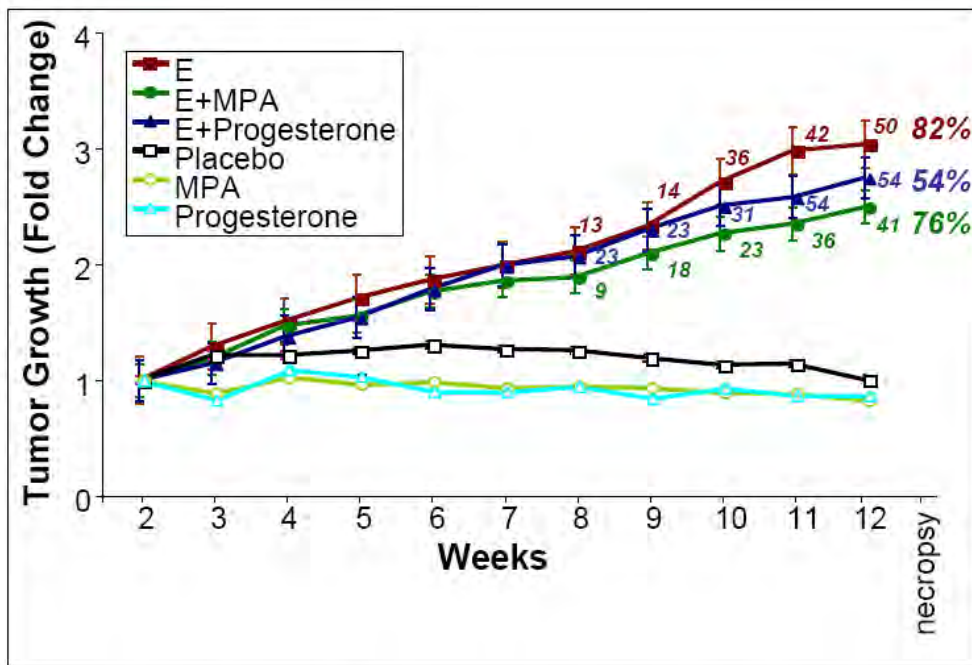
Figure 1: MCF7+ZsGreen tumors were grown with either E (n=15), E+MPA (n=25), E+P (n=14), placebo (n=6), MPA (n=7), or P (n=3) for 12 weeks in ovariectomized nude mice. Tumor area and presence of metastases were assessed by weekly whole-body imaging and by intravital imaging at necropsy. The percentage of mice with LN metastasis is indicated at each time point.

Task 3. The third task in my approved statement of work is to determine hormonal influence on tumor lymphangiogenesis. In my year-one first-author publication I show that estradiol dependent tumor growth correlates with intratumoral lymphangiogenesis (3); intratumoral lymphatic vessels were only identified in estradiol treated MCF-7 tumors. Peritumoral LVs were found surrounding nearly all tumors, regardless of hormone treatment, and likely derived from the normal lymphatic vasculature present in the mammary gland. To further investigate hormonal roles in lymphatic vessel development, during year two of my funding, I set up collaborations with Dr. Kenneth Korach at the National Institutes of Environmental Health Sciences and Dr. Darryl Russell at the University of Adelaide (South Australia). Through RT-PCR analyses we found that ER alpha is required in the ovary for proper lymphatic remodeling that occurs after ovulation, whereas ER beta has no role in this process. This is the first demonstration that estrogen controls lymphangiogenesis. This project is being expanded upon by my collaborators and we expect a publication within the next year. **These studies complete task 3.**

Ongoing studies. The approved statement of work is complete.

Key Research Accomplishments

- Developed a model of fluorescent estrogen-dependent LN metastasis (Harrell et al., CanRes 2006, Figures 1-3).
- Identified that tumor growth correlates with LN spread (Harrell et al., CanRes 2006, Figure 3).
- Found that estrogen-dependent tumor growth stimulates intratumoral lymphangiogenesis (Harrell et al., CanRes 2006, Figure 4).
- Found that the LN microenvironment increases the proliferation rate of cancer cells (Harrell et al., CanRes 2006, Figure 5).
- Found that the LN microenvironment increases ER expression and decreases ER function (Harrell et al., CanRes 2006, Figure 6).
- Identified that cells that express CD44 are selected for lymphatic metastasis (Harrell et al., CanRes 2006, Figure 7).
- Identified that globally there is less estrogen regulation of genes in LNs as compared to primary tumors (Harrell et al., CanRes 2006, Figure 3).
- Identified specific genes that are regulated by the tumor microenvironment, by hormones, or by both (Harrell et al., CanRes 2006, Figures 3-6).
- Determined that both medroxyprogesterone acetate (MPA) and progesterone have no influence on MCF7 breast tumor growth or metastasis (Figure 1)

Reportable Outcomes

1- Manuscripts See NIH Biosketch in appendices.

2-Degree Completion & Future Employment

My thesis was completed in the summer of 2007. Upon graduation I stayed in the Horwitz lab to complete this project and to set-up my postdoctoral lab. I have since accepted an offer to postdoc with Dr. Charles M. Perou at the University of North Carolina, and will start in his lab towards the end of 2008. I am currently a finalist for the DOD Era of Hope Postdoctoral Award.

Conclusions

The three years of funding for the predoctoral grant BC050889 were highly successful. The research conducted yielded exciting results and further tested the first known reliable model of ER+ breast cancer metastasis *in vivo*. This model and methods have since led to the establishment of collaborations with numerous investigators internationally. Results found that there are differences in estrogen responsiveness in breast tumors compared to the matched LN metastases, suggesting that aromatase inhibitors and other estrogen/ER mediated therapies may be differentially affecting cancer cells—dependent on their tissue location. Also, I showed that laser-capture microarray analysis is more sensitive and accurate than whole-tissue analysis. These studies have furthered my career and yielded opportunities I never thought would be possible.

References

1. Harrell JC, Dye WW, Harvell DM, Pinto M, Jedlicka P, Sartorius CA, Horwitz KB. Estrogen insensitivity in a model of estrogen receptor positive breast cancer lymph node metastasis. Cancer Res. 2007 Nov 1;67(21):10582-91.

2. Harrell JC, Dye WW, Harvell DM, Sartorius CA, Horwitz KB. Contaminating cells alter gene signatures in whole organ versus laser capture microdissected tumors: a comparison of experimental breast cancers and their lymph node metastases. Clin Exp Metastasis. 2008;25(1) 81-8.

3. Harrell JC, Dye WW, Allred DC, Jedlicka P, Spoelstra N, Sartorius CA, and Horwitz KB. Estrogen Receptor Positive Breast Cancer Metastasis: Altered Hormonal Sensitivity and Tumor Aggressiveness in Lymphatic Vessels and Lymph Nodes. Cancer Research, 2006; 66: (18). September 15, 2006.

Appendices

1. NIH Biosketch.
2. Bibliography of publications and meeting abstracts from the award period.

Name: **Joshua "Chuck" Christopher Harrell**   Current Title: Postdoctoral Fellow

EDUCATION/TRAINING

INSTITUTION AND LOCATION	DEGREE	YEAR(s)	FIELD OF STUDY
North Carolina State University-Raleigh, NC, US	BS	2000	Biological Sciences
University of Colorado Health Sciences Center-Aurora, CO, US	PhD	2007	Cell & Developmental Biology; Cancer Research

RESEARCH AND PROFESSIONAL EXPERIENCE

University of North Carolina at Chapel Hill, NC, USA
  Postdoctoral Fellow (7/2008)
University of Colorado Health Sciences Center, Aurora, CO, USA
  Postdoctoral Fellow (5/2007-6/2008)
  Graduate Student (8/2002-5/2007), Doctoral Candidate (11/2005-5/2007)
University of Adelaide, Adelaide, South Australia
  United States National Science Foundation EAPSI Participant (6/2007-8/2007)
National Institutes of Environmental Health Sciences, Research Triangle Park, NC, USA
  Intramural Recreational Training Award (12/2000-7/2002)
  Undergraduate Internship (9/1998-6/1999, 8/1999-12/2000)
North Carolina Division of Marine Fisheries, Morehead City, NC, USA
  NC State Government Undergraduate Summer Internship Program (6/1999-8/1999)

AWARDS

United States National Science Foundation East Asia and Pacific Summer Institute in Australia (6/2007-8/2007)
1st place poster: 2006 UCHSC Department of Medicine Research Day (10/2006)
C. Werner and Kitty Hirs 2006 Research Award for UCHSC PhD Student Travel to National Meetings (8/2006)
2nd place poster: 2006 Cell and Developmental Biology and Reproductive Sciences Annual Retreat (8/2006)
United States DOD Breast Cancer Predoctoral Training Award (3/2006-3/2009)
1st place poster: 2005 Cell and Developmental Biology and Reproductive Sciences Annual Retreat (9/2005)
Avon Foundation Scholar (2004-2007)
United States DOD Breast Cancer Training Grant (9/2003-8/2004)

RESEARCH CONFERENCES ATTENDED & INVITED SEMINARS

2007 Seminar-National Institutes of Environmental Health Sciences, Research Triangle Park, NC
2007 Seminar-University of North Carolina, Chapel Hill, NC
2007 Seminar-University of Adelaide, Adelaide South Australia.
2007 Seminar-Prince Henry's Medical Institute, Melbourne, Victoria Australia.
2007 Poster Presenter-Keystone Symposia: Host cell response to the cancer cell, Keystone, CO, US
2006 Poster Presenter-Gordon Conference: Lymphatic function and disease, Les Diablerets, Switzerland
2005 Speaker-25th Annual San Antonio Breast Cancer Symposia, San Antonio, TX, US
2003 Attendee-Keystone Symposia-Nuclear Receptors: Steroid Hormones, Keystone, CO, US

PEER REVIEWED JOURNALS

Molecular Cancer Research, Journal of Clinical Chimica Acta

PUBLICATIONS

Horwitz KB, Dye WW, **Harrell JC**, Kabos P, Sartorius CA. Steroid Receptor Negative Breast Cancer Stem Cells are Expanded by Progesterone and Generate Receptor Positive Tumor Cell Populations. PNAS, Apr 15;105(15):5774-9

Christenson KL, Micalizzi DS, Coletta RD, Jedlicka P, **Harrell JC**, Horwitz KB, Billheimer D, Heichman K, Welm A, Ford HL. The developmental regulator Six1 promotes an epithelial to mesenchymal transition, induces metastasis, and predicts poor prognosis in many human cancers. Submitted June, 2008.

Harrell JC, Dye WW, Harvell DM, Sartorius CA, Horwitz KB. Contaminating cells alter gene signatures in whole organ versus laser capture microdissected tumors: a comparison of experimental breast cancers and their lymph node metastases. Clin Exp Metastasis, 2008;25(1):81-8.

Harrell JC, Dye WW, Harvell D, Pinto M, Sartorius CA, Horwitz KB. Estrogen insensitivity in a model of estrogen receptor positive breast cancer lymph node metastasis. Cancer Research, 2007 Nov 1;67(21):10582-91.

Harrell JC, Sartorius CA, Dye WW, Jacobsen BM, Horwitz KB. ZsGreen labeling of breast cancer cells to visualize metastasis. Clontechniques. April 2007.

Massart F, Federico G, **Harrell JC**, Saggese G. Thyroid outcome during long-term gonadotropin-releasing hormone agonist treatments for idiopathic precocious puberty. In press, Journal of Adolescent health. 2007.

Harrell JC, Dye WW, Allred DC, Jedlicka P, Spoelstra NS, Sartorius CA, Horwitz KB. Estrogen receptor positive breast cancer metastasis: altered hormonal sensitivity and tumor aggressiveness in lymphatic vessels and lymph nodes. Cancer Research. 2006 Sep 15;66 (18):9308-15.

Jacobsen BM, **Harrell JC**, Jedlicka P, Borges VF, Varella-Garcia M, Horwitz KB. Spontaneous fusion with, and transformation of mouse stroma by, malignant human breast cancer epithelium. Cancer Research. 2006 Aug 15;66 (16):8274-9.

Hewitt SC, **Harrell JC**, Korach KS. Lessons in estrogen receptor biology from knockout and transgenic animals. Annual Review of Physiology. Volume 67, 2005: 285-308.

Massart F, **Harrell JC**, Federico G, Saggese G. Human breast milk and xenoestrogen exposure: a possible impact on human health. J Perinatol. 2005 Apr; 25(4):282-8.

Melvin VS, **Harrell C**, Adelman JS, Kraud WL, Churchill M, Edwards DP. The role of the C-terminal extension (CTE) of the estrogen receptor alpha and beta DNA binding domain in DNA binding and interaction with HMGB. J Biol Chem. 2004 Apr 9;279(15):14763-71.

Korach KS, Emmen JM, Walker VR, Hewitt SC, Yates M, Hall JM, Swope DL, **Harrell JC**, Couse JF. Update on animal models developed for analyses of estrogen receptor biological activity. J Steroid Biochem Mol Biol. 2003 Sep:86(3-5):387-91.

Swope D, **Harrell JC**, Mahato D, Korach KS. Genomic structure and identification of a truncated variant message of the mouse estrogen receptor alpha gene. Gene. 2002 Jul 10;294(1-2)239-47.

Hewitt SC, Bocchinfuso WP, Shai J, **Harrell C**, Koonce L, Clark J, Myers P, Korach KS. Lack of ductal development in the absence of functional estrogen receptor alpha delays mammary tumor formation induced by transgenic expression of ErbB2/neu. Cancer Research. 2002 May 15;62(10):2798-805.

Swope DL, Castranio T, **Harrell JC**, Mishina Y, Korach KS. AF-2 knock-in mutation of estrogen receptor alpha: Cre-loxP excision of a PGK-neo cassette from the 3'UTR. Genesis. 2002 Feb;32(2):99-101.

MEETING ABSTRACTS

2006 Gordon Conference: Molecular Mechanisms in Lymphatic Function & Disease. September 3, 2006-September 8, 2006. Les Diablerets, Switzerland. *Characterizing a model of estrogen-dependent lymph node metastasis.*

2007 Keystone Symposia: Host cell Interaction and Response to the Cancer Cell. January 21-26, 2007. Keystone, Colorado. *Characterizing a model of estrogen-dependent lymph node metastasis.*

Estrogen Receptor Positive Breast Cancer Metastasis: Altered Hormonal Sensitivity and Tumor Aggressiveness in Lymphatic Vessels and Lymph Nodes

Joshua Chuck Harrell,[1,3] Wendy W. Dye,[1] D. Craig Allred,[4] Paul Jedlicka,[2] Nicole S. Spoelstra,[1] Carol A. Sartorius,[1] and Kathryn B. Horwitz[1,2,3]

Departments of [1]Medicine, [2]Pathology, and [3]Program in Reproductive Sciences, University of Colorado Health Sciences Center, Aurora, Colorado; and [4]Breast Center, Baylor College of Medicine, Houston, Texas

Abstract

Breast cancers commonly spread to lymph nodes (LNs). If the primary tumors are estrogen receptor (ER) and/or progesterone receptor (PR) positive, then the likelihood that LN metastases express receptors exceeds 80%. However, due to lack of ER+ models, little is known about the role of hormones in breast cancer spread or the effects of the LN microenvironment on hormone responsiveness. We have developed metastasis models using ZsGreen labeled MCF-7 and T47D human breast cancer cells. Tumors are tracked in living mice by whole-body imaging, and macrometastases or micrometastases are detected by intravital imaging or fluorescence microscopy. Tumor growth is estrogen dependent and required for intratumoral lymphangiogenesis. Seventy-five percent of all tumors and >95% of larger tumors generate LN metastases. Occasionally more distant metastases are also observed. "Triads" of primary tumors, tumor-filled draining lymphatic vessels, and tumor-filled LNs from the same mouse show that (_a_) proliferation, as measured by 5-bromo-2′-deoxyuridine uptake, is higher in the LN than in the primary tumor. (_b_) High ER levels are extensively down-regulated by estradiol in primary tumors. However, there is partial failure of ER down-regulation in LNs associated with (_c_) reduced PR expression. This suggests that ER are dysfunctional in the LN microenvironment and perhaps hormone resistant. (_d_) CD44 is sparsely expressed in primary tumor cells but homogeneously overexpressed in cells transiting the lymphatics and populating LNs. We hypothesize that CD44 expression targets tumor cells for transport to, and uptake in, LNs. If so, the CD44 pathway could be targeted therapeutically to slow or prevent LN metastases. (Cancer Res 2006; 66(18): 9308-15)

Introduction

Advanced breast cancer kills >40,000 American women each year and 10 times that number worldwide (1, 2). Seventy to 80% of primary breast cancers are estrogen receptor (ER) and/or progesterone receptor (PR) positive and considered to be hormone responsive (3). Importantly, if the primary tumors are ER+, >80% of lymph node (LN) metastases and 65% to 70% of distant metastases retain their receptors (4–6). Despite this, little is known about the role, if any, of estrogens or progestins in influencing the spread of tumor cells from the primary site, or their deposition and growth at metastatic sites.

This lack of information is due, in part, to a lack of ER+ experimental metastasis models. The three ER+ human breast cancer cell lines most widely used for orthotopic xenograft studies are MCF-7, T47D, and ZR75 cells (7). They develop tumors in mammary glands of nude mice in response to estradiol supplementation (8, 9). However, most reports state that such tumors are poorly invasive and rarely, if ever, metastasize (9). Indeed, most metastasis models do not use these cells, relying instead on ER− cell lines like MDA-231, MDA-435 (10) and similar cells that express putative aggressiveness markers and do metastasize in nude mice. Other studies analyze only late stages of metastases by injecting ER− tumor cells directly into the circulation (11). Alternative approaches for studying tumor aggressiveness from orthotopic sites with ER+ breast cancer cells involve their modification to overexpress oncogenes like v-Ha-ras (12) or HER-2/neu (13), growth factors like vascular endothelial growth factor (14) or fibroblast growth factor (15), or transcription factors like Id-1 (16) or Fra-1 (17), in an effort to enhance tumor progression while suppressing estrogen-dependent behavior (18). We considered, however, that if the clinical data cited above are a guide, it should not be necessary to suppress hormone responsiveness to achieve a metastatic phenotype.

Observation of metastasis can be difficult, especially if few cells are involved or appropriate target organs are unexplored. The development of fluorescent proteins to genetically tag living cells has greatly increased the likelihood that metastases will be visualized (19). Indeed, jellyfish green fluorescent protein has been widely used for studies of ER− cells (20). Recently, a set of coral reef fluorescent proteins were identified that require no cofactors or substrates (21). These fluors have been modified to produce variants with even brighter fluorescence and enhanced emission characteristics than green fluorescent protein, and codon usage has been modified to optimize their mammalian expression. Among these fluors, ZsGreen has unique excitation and emission patterns within the visible spectrum.

This report reevaluates the metastatic potential of ER+ MCF-7 and T47D human breast cancer cells in orthotopic mouse tumors using ZsGreen as a sensitive new tracking method. Cells stably expressing this fluor and grown as xenografts in mammary glands of nude mice were absolutely estrogen dependent. Tumor fluorescence was stable and superficial LN metastases were monitored in living mice. At necropsy, stably fluorescent metastatic cells were reliably detected microscopically in lymphatics in local and distant LNs and, occasionally, in distant organs. If the primary tumors were ER+ and PR+, then metastases retained receptors, but their expression levels and that of the proliferation marker

5-bromo-2′-deoxyuridine (BrdUrd) were modified by the LN microenvironment. In addition, the hyaluronan receptors, CD44, which control chemotactic behavior of tumor cells (22), were up-regulated in cells transiting the lymphatics and retained in LNs. These data suggest strategies for suppressing LN metastases and indicate that once in the LNs, tumor cells have reduced hormonal sensitivity.

Materials and Methods

Cell lines. MCF-7 cells were originally purchased from American Type Culture Collection (Manassas, VA). Generation of T47D cells that express one PR isoform was previously described (23), and in the present study PR-B expressing T47D cells were used exclusively. The ZsGreen-N1 expression vector, PT-67 packaging cell line, and pLNCX2 retroviral vector were purchased from Clontech/Becton Dickinson (Franklin Lakes, NJ). Fluorescent retroviral vectors were generated by cloning the DNA coding sequence of ZsGreen into the pLNCX2 vector using the restriction enzymes *Hin*dIII and *Not*I and T4 ligase. Plasmids were then transfected into PT-67 packaging cells with a standard calcium phosphate protocol. Stable retrovirus producing cells were selected by 2 weeks of treatment with 500 µg/mL G418. MCF-7 or T47D cells were plated at ∼ 20% confluence and incubated in filtered, virus-containing supernatant. Cells were serially transduced two to three times for 24 hours each round, at which point they exhibited heterogeneous green expression. Cells were then subjected to G418 selection, followed by aseptic fluorescence associated cell sorting (FACS), to isolate a homogeneously bright green subpopulation. These cells were returned to culture and remained bright green through multiple passage generations. Expression of ER and PR in the selected cells was confirmed by immunohistochemistry (see below).

Xenograft tumor growth and metastases. All animal procedures were done under a protocol approved by the University of Colorado Institutional Animal Care and Use Committee. Ovariectomized female athymic *nu/nu* mice were obtained from Harlan Sprague-Dawley (Indianapolis, IN) at 5 to 6 weeks of age. To establish tumors, animals were anesthetized with Avertin and injected into the opening of the lactiferous duct of the abdominal mammary gland with 1 million ZsGreen-expressing MCF-7 or T47D cells in 100% Matrigel (Becton Dickinson). Mice were also implanted with silastic pellets containing cellulose (10 mg) or 17β-estradiol (2 mg + 8 mg cellulose) as previously described (24). Tumor size was recorded weekly with a digital caliper. Fluorescent whole-body imaging was done weekly (Illumatool 9900, Lightools Research, Encinitas, CA). Two hours before necropsy 100 mg/kg BrdUrd in PBS was injected i.p. At the end of the study, mice were euthanized by CO_2 asphyxiation and fluorescent intravital optical imaging was done by coupling the Illumatool with an Olympus (Melville, NY) SZ-61 dissecting microscope and Olympus C-5050 digital camera. Organs were removed for histology, immunohistochemistry, and fluorescence microscopy.

Histology, immunohistochemistry, and fluorescence microscopy. Organs were fixed in 4% paraformaldehyde overnight, paraffin embedded, and cut into 4- to 5-µm sections. After high-temperature antigen retrieval in citrate buffer, sections were stained with H&E. Immunohistochemistry was done on parallel sections for 1 hour at room temperature, with primary antibodies directed against ER (6F11; Vector Labs, Burlingame, CA), PR (1294; Dako, Carpinteria, CA), BrdUrd (Becton Dickinson), CK18 (Calbiochem, La Jolla, CA), CK8/CK18 (5D3; Novocastra, Newcastle-upon-Tyne, United Kingdom), LYVE-1 (Upstate, Lake Placid, NY), Prox-1 (Abcam, Cambridge, MA), or CD44 (Ab4; NeoMarkers/Labvision, Fremont, CA). Bound primary antibodies were detected with horseradish peroxidase (HRP)–conjugated goat anti-mouse and/or goat anti-rabbit secondary antibodies (Envision HRP; Dako). Sections were counterstained with hematoxylin and mounted. For immunofluorescence microscopy, goat anti-rabbit Alexa Fluor 555 (red) and goat anti-mouse Alexa Fluor 488 (green) secondary antibodies were used (Alexa Fluors; Invitrogen, Carlsbad, CA). For fluorescence microscopy, tissues were processed and sectioned as above, paraffin was removed with xylene, and then mounted with fluoromount G (EMS, Hatfield, PA).

Statistical analyses. Data from immunohistochemistry experiments were collected by an investigator who photographed tissue sections and a blinded investigator that counted cells from random fields of stained sections using Image Pro software version 4.5.0.29 (Media Cybernetics, Inc., Silver Spring, MD). Each field was quantified either as a percentage of positively stained cells or an Allred score (ref. 25; percent of labeled cells added to the intensity of immunolabeling). Fields from the same tissue section were averaged and SPSS software version 12.0.2 (SPSS, Inc., Chicago, IL) was used to analyze the data. A Mann-Whitney U test was used to compare BrdUrd-positive HRP-stained cells in independent, nonparametric samples of estradiol- and placebo-treated mouse tumors. Paired t test was used to compare fluorescent-stained cells positive for CK18/BrdUrd, ER, or PR of tumor, LN, and associated lymphatic embolus triad from one mouse to those of other triads from other mice. A marginal homogeneity test was used to compare ER+ and PR+ HRP expression on Allred scores in nonparametric mouse triad samples. For all tests, $P < 0.05$ was considered significant.

Results

An *in vivo* model of estrogen-dependent human breast cancer LN metastasis. The ER+ human breast cancer cell lines MCF-7 and T47D are commonly used to study the biology of estrogen action *in vitro*. These cells also grow as estrogen-dependent xenografts in nude mice (8, 24, 26), but most published reports state that orthotopic tumors fail to metastasize. Because, clinically, ER+ tumors metastasize frequently (4–6), we decided to reevaluate the metastatic potential of ER+ human breast cancer cells in xenografts using sensitive new tracking methods. To this end, MCF-7 and T47D cells were retrovirally transduced with ZsGreen, G418 selected, and the brightest green subpopulation was isolated by FACS sorting. Confocal imaging showed that ZsGreen was highly expressed in both cell types, in the cytoplasm and nuclei (not shown). Intense fluorescence is maintained through multiple passages, the fluor is nontoxic, and photobleaching studies show that ZsGreen, a coral reef protein, is much brighter and more photostable than green fluorescent protein, a jellyfish protein (not shown).

Visualizing lymphovascular tumor cell spread. One million fluorescent tumor cells in Matrigel were injected into the lactiferous duct of the abdominal (#4) mammary gland of 5- to 6-week-old, ovariectomized *nu/nu* mice supplemented with an estradiol-releasing silastic pellet (24). This injection route led to formation of well-circumscribed tumor cell nodules distant from the subiliac LN in the gland, as shown by a whole mount 3 days after injection (Fig. 1*A, top*). In contrast, whole mount of a tumor at 12 weeks shows the subiliac LN, still physically distinct from the primary tumor but already highly involved with tumor cells (Fig. 1*A, bottom*).

This protocol was used to track the spread of ER+ tumors beyond the #4 mammary gland using whole-body imaging of live mice done weekly. Figure 1*B* shows an image of tumor tracks photographed through the skin of an intact mouse at 12 weeks. Bright green bilateral tumors are present in mammary gland #4 at the groin, and both subiliac mammary gland LNs contain tumor cells. Also clearly visible are tumor cell tracks in the epigastric collecting lymphatic vessels (LV) draining the tumor cranially on the right, as well as tumor cells in the right axillary LN. Similarly, three distinct green fluorescent clusters of tumor cells are faintly seen in the left lymphatics and axillary LN.

At sacrifice, intravital fluorescence microscopy was used to examine tumor spread to visceral tissues as shown in Fig. 1*C* and *D*. An axillary LN micrometastasis is seen in one mouse at 12 weeks (Fig. 1 *C, left*) and a fully involved LN metastasis in another mouse at 12 weeks (Fig. 1*C, right*). Figure 1*C* also shows the afferent LV full of tumor cells, with the parallel epigastric vein devoid of such cells. Tumor cells also spread medially to the abdomen. Shown in Fig. 1*D* is early invasion into a periaortic LN
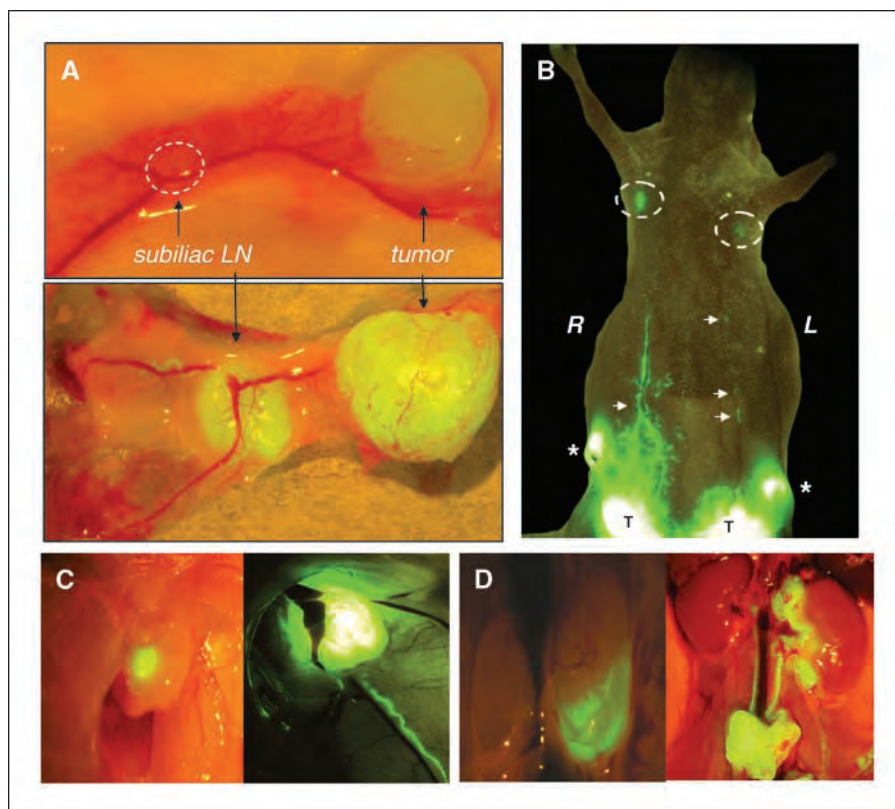
Figure 1. Whole-body and intravital images of ZsGreen-expressing ER+ human breast cancer cells and their LN metastases. *A,* excised abdominal mammary gland from a 3-day-old MCF-7 tumor, in relation to the subiliac LN (*top, dashed circle*), and from a 12-week-old MCF-7 tumor with a LN metastasis at a similar site (*bottom*). *B,* whole-body image showing bilateral T47D tumors (*T*), subiliac LN metastases (*), collecting LV (*arrows*), and axillary LN macrometastases (*right*) and micrometastases (*left; dashed circles*). *C,* intravital image of MCF-7 axillary LN metastasis showing a micrometastasis (*left*) and a macrometastasis (*right*) with a collecting LV draining into it. *D,* intravital image of an MCF-7 metastasis to the left para-aortic LN (*left*) and more progressive disease showing coalesced left and right para-aortic LNs and further tumor spread caudally to the renal LNs (*right*).

(*left*) and also much more extensive metastases to periaortic and renal LNs (*right*).

Bilateral tumor-filled lymphatic tracks exiting a primary tumor are clearly seen in Fig. 2*A*. LV full of tumor cells extend both cranially and medially from the tumor. It is possible that the tortuously branching network of lymphatics exiting the tumor cranially represents lymphangiogenesis. A higher-power view of the laterally branching iliac LV shows that the tumor cells within it coalesced into emboli rather than moving as discrete cells. In response to mechanical pressure applied either to the tumor or the efferent lymphatic root during dissections, fluorescent emboli in collecting lymphatics can often be seen moving into their draining LN (not shown). This has implications for the order in which breast surgical procedures and sentinel node biopsies are done. In general,
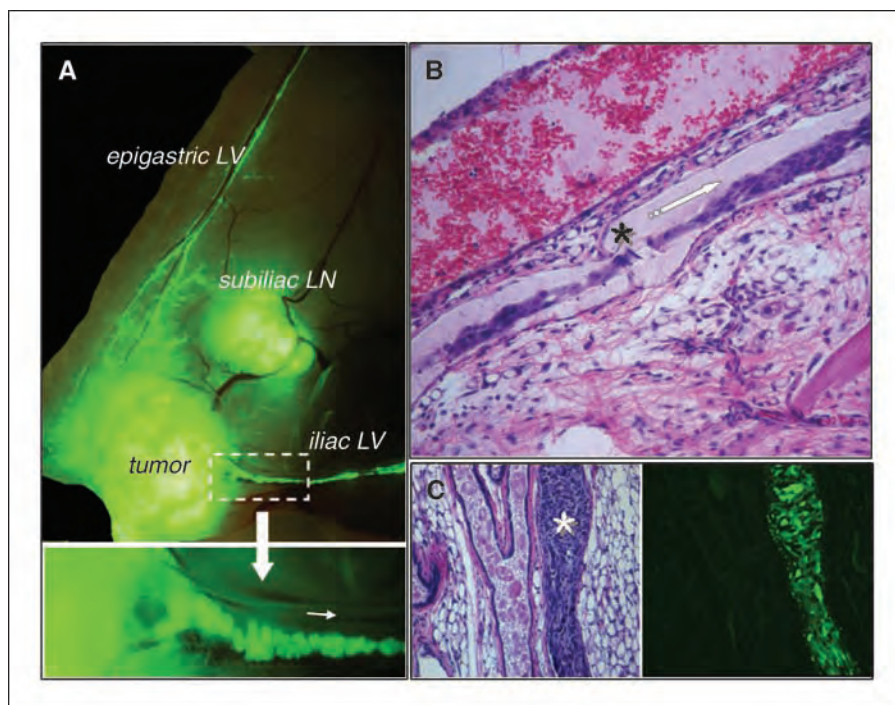
Figure 2. Identification of cancer cells in LVs. *A, top,* intravital image of a T47D tumor, showing its metastasis to the subiliac LN, and cells moving through the epigastric and iliac LVs. *Bottom,* higher magnification of the iliac LV showing clusters of cells moving inwards toward the para-aortic LNs. *B,* the isolated epigastric LV from (*A*) showing cancer cells moving through a collecting valve (*) in route to the axillary LN. *C, left,* an isolated collecting LV full of MCF-7 cancer cells (*) paralleling a milk duct. *Right,* a serial section confirms the identity of the cancer cells and shows maintenance of ZsGreen fluorescence after tissue processing into paraffin blocks.

tumor cell spread to the superficial LNs is restricted to the side of the body containing the primary tumor, and spread to deeper LNs becomes bilateral with progressive disease (Fig. 1D). Directional valves (*asterisk*) within the LV do not inhibit tumor cells moving through LVs, as shown in Fig. 2B. Lastly, fluorescence microscopy can be used to analyze clinicopathologic features of tumors and their metastases. Importantly, ZsGreen fluorescence is maintained throughout the histologic fixation process. Figure 2C shows the H&E stain of a collecting LV filled with tumor cells within the mammary gland fat pad. A milk duct runs alongside it. Fluorescence microscopy of a serial section confirms that tumor cells are restricted to the LV.
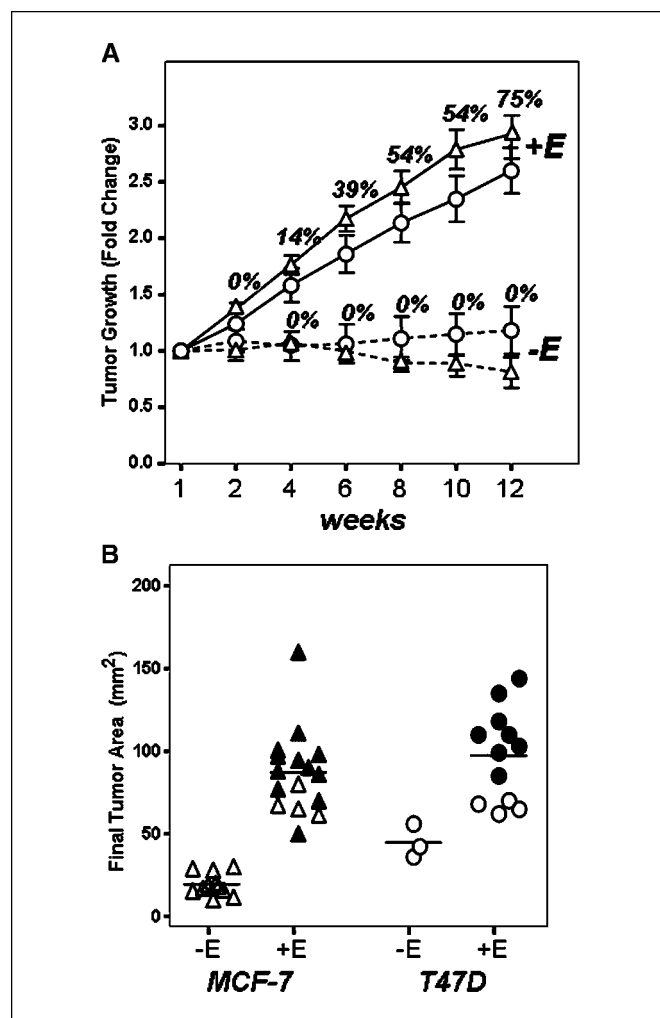
Estrogen-dependent tumor growth and rate of LN metastases. Figure 3 summarizes the primary tumor growth pattern of MCF-7 and T47D cells during 12 weeks of observation and the extent of LN metastasis as assessed by whole-body and intravital imaging. Growth from both cell types is estradiol dependent, with tumors nearly tripling in size in ~12 weeks (Fig. 3A). Both MCF-7 and T47D tumors produce LN metastases at the same rate, which increases with time and tumor size. At 2 weeks, no metastases occurred. By 4 weeks, ~14% of tumors generated LN metastases. This increased to ~75% at 12 weeks. Development of LN metastases seems to be size dependent (Fig. 3B). A separate time-course study of tumors grown for 1, 6, or 12 weeks showed that metastases to superficial subiliac and axillary LN, or to deeper visceral lateral iliac and aortic lumbar LN surrounding the aorta and kidneys, tend to occur at the same rate.

Estradiol and LV development. Because only estradiol-treated tumors yielded LN metastases, we next studied the effects of estradiol on tumor-associated LV development. For these studies, tumors were grown with or without estradiol supplementation for short term (3-10 days) or long term (6-12 weeks) and LV were quantified with lymphatic-specific LYVE-1 and Prox-1 (not shown) antibodies. Peritumoral LVs were identified in both treatment groups and likely represent lymphatics found adjacent to veins and arteries in the normal mouse mammary gland (Fig. 4). Intratumoral LVs were not seen after short-term estradiol treatment or in the estradiol-deprived dormant tumors. Fifty-eight percent of long-term estradiol-treated tumors contained intratumoral LVs (Fig. 4). ZsGreen fluorescence was quenched during the immunolabeling process, allowing for double immunostaining with anti-LYVE and anti-BrdUrd antibodies (Fig. 4) to assess the proliferation state of the LV. This procedure showed the LVs to be BrdUrd positive, suggesting that lymphangiogenesis was occurring. However, double labeling for LYVE and ER expression showed absence of ER in the LVs (not shown). We conclude that LV proliferation, although restricted to the estradiol-dependent growing tumors, is either not itself estradiol dependent or is occurring in response to paracrine signals from surrounding ER+ tumor cells.

The triad of primary tumor, lymphatic emboli, and LN metastases: proliferation. Our ability to dissect a primary tumor, its draining lymphatic collecting duct filled with tumor cells, and the downstream tumor-filled LN, from the same mouse, allows assessment of the role of the microenvironment in tumor cell proliferation and steroid receptor expression. BrdUrd uptake, measured with BrdUrd primary antibodies coupled to a HRP or a green fluorescent secondary antibody, was used to assess the proliferation rate of cells in these different compartments. In the absence of estradiol, tumor cells at the injection site remain viable and proliferate slowly with a labeling index <7% (Fig. 5A), but at a rate insufficient to elicit an overall increase in tumor

size at 12 (Fig. 3) or 16 to 20 weeks (not shown). These dormant tumors yield no LN metastases. In the presence of estradiol, primary tumors exhibit extensive BrdUrd uptake with a labeling index of ~20%.

To accurately quantify dispersed tumor cells and eliminate the contribution of proliferating normal host cells, tumor cells were immunolabeled with CK18 and a red secondary antibody. In this case, proliferating cells were quantified with anti-BrdUrd and a green fluorescent secondary antibody, and some sections were also counterstained with blue 4′,6-diamidino-2-phenylindole (DAPI). Figure 5B shows two "triads" of tumor, LV and LN. Each triad came from the same mouse; the two sets were taken from two different mice. In triad 1, although the primary tumor cells have a high labeling index, proliferation in the LV embolus is low and mainly restricted to cells at the periphery, and in the LN, tumor cells are present only in the subcapsular sinus. The remainder consists of normal DAPI-stained LN cells (some of

Figure 3. Estrogen-dependent tumor growth is required for LN metastasis. *A,* MCF-7 (*triangles*) and T47D (*circles*) tumors were grown either with (+E) or without (−E) estradiol for 12 weeks in ovariectomized nude mice. Tumor area was quantified with digital calipers and presence of metastases was assessed by weekly whole-body imaging and by intravital imaging at necropsy. The percent of mice with LN metastasis is indicated at each time point. *B,* tumor area at necropsy as assessed by the diameter in two dimensions. *Filled symbols,* tumors from which metastasis developed; *open symbols,* tumors that did not generate metastases.
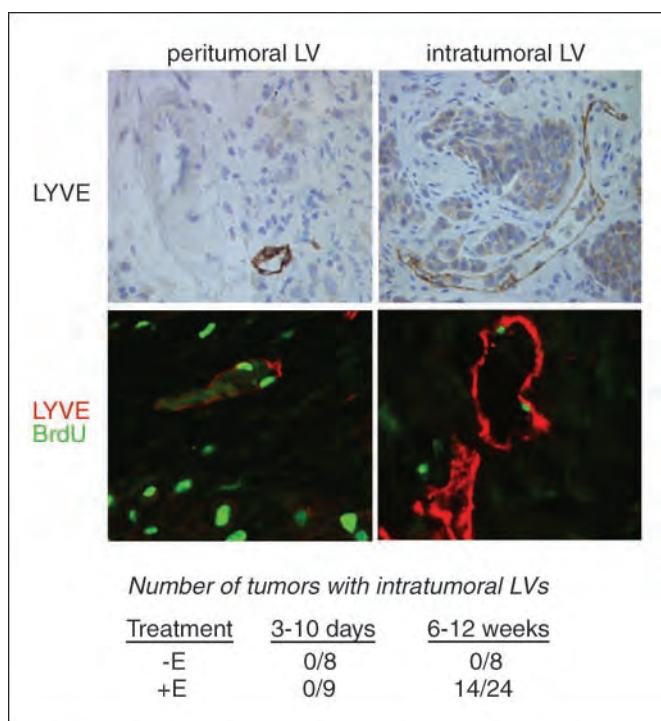
Figure 4. Assessment of tumor-associated lymphatics and lymphangiogenesis. Tumors from 3- to 10-day-old or 6- to 12-week-old placebo-treated (−E) and estradiol-treated (+E) ovariectomized mice were paraffin embedded. *Top,* sections (5 μm) were probed for LVs with an anti-LYVE-1 antibody and an HRP-labeled secondary antibody. *Bottom,* sections were probed by dual fluorescence immunohistochemistry with mouse anti-BrdUrd and rabbit anti-LYVE primary antibodies, followed by goat anti-mouse (*green*) and goat anti-rabbit (*red*) secondary antibodies, to identify lymphatics in S phase. The table quantifies the results.

which are also undergoing cell division). Triad 2 exhibits a different pattern, with extensive proliferation in the primary tumor and throughout the LV emboli, and the LN is highly involved with rapidly proliferating tumor cells.

Figure 5*C* quantifies all proliferation data. It shows, first, that the two methods of assessing BrdUrd uptake yielded similar results (compare the two +E "tumor" sets—one assessed with HRP and the other with dual BrdUrd/CK18 immunohistochemistry). As expected, compared with dormant controls, estradiol-treated primary tumors exhibit a statistically significant increase in proliferation rate from ∼7 to ∼20%. And, compared with the primary tumors, metastatic cells in the LN microenvironment have a statistically significant ($P = 0.003$) further increase to ∼27%. Proliferation rates of embolic cells in the LV were variable and not statistically different from the other two compartments, although they tended to resemble those in the primary tumor more closely.

The triad of primary tumor, lymphatic emboli, and LN metastases: ER and PR. ER and PR immunohistochemistries for two sets of vehicle versus estradiol-treated triads using MCF-7 derived tumors show the heterogeneity observed (Fig. 6). In the absence of estradiol, levels of ER in tumors are always high. Estradiol treatment leads to extensive tumor ER down-regulation. ER tend to remain low in the LV and LN of Fig. 6 (*top*) but are somewhat restored in the LN of the second triad (*bottom*). No PR are expressed without estradiol induction. Estradiol treatment leads to heterogeneous PR expression in tumors, which tends to decrease in LV and LN of the same mouse. Quantitation of PR

data from several mice is shown in Fig. 6. There is a clear trend of decreased PR expression as cells spread into LV and LN ($P = 0.052$). A second experiment (not shown) using fluorescent immunohistochemistry for ER and PR showed a similar trend of reduced PR between five tumors and their matched LNs ($P = 0.09$). Each immunohistochemical procedure showed a
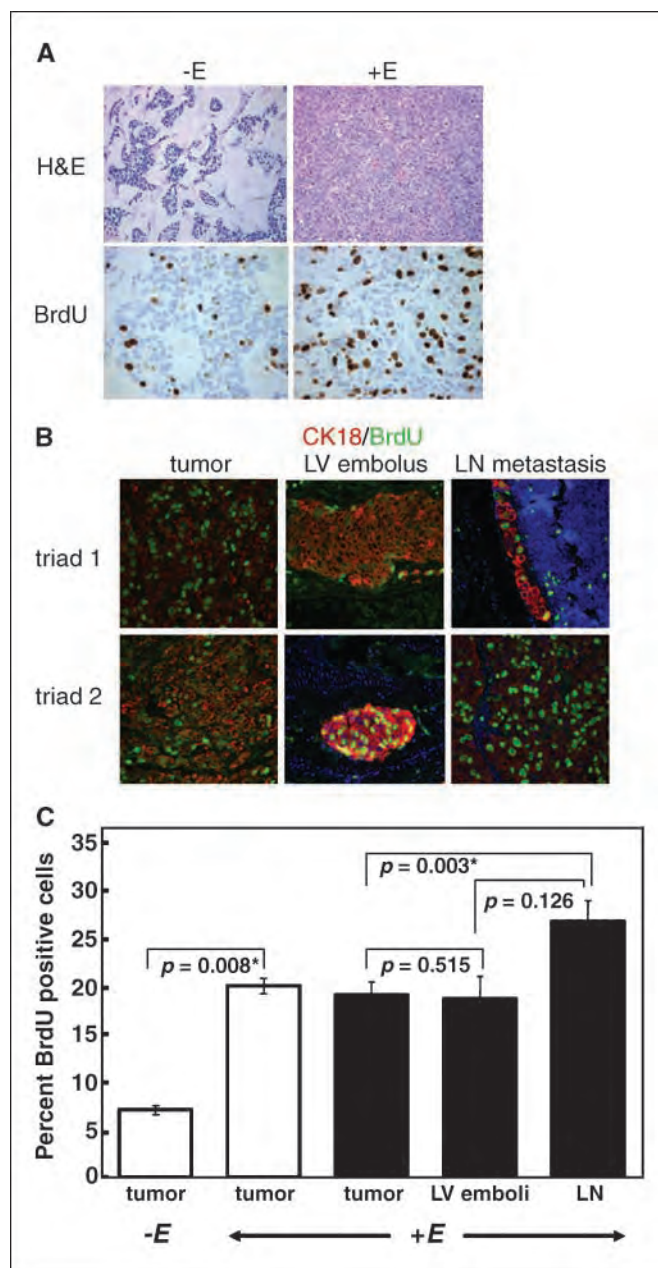
Figure 5. Assessment of tumor proliferation in MCF-7 tumors, LV emboli, and LN metastases. *A,* ovariectomized mice bearing MCF-7 tumors were treated for 12 weeks with placebo (−E) or estradiol (+E). Tumors were paraffin embedded, sectioned, and stained with H&E or analyzed by BrdUrd-HRP immunohistochemistry. *B,* dual fluorescence immunohistochemistry for cytokeratin 18 (*red*) and BrdUrd (*green*) of estradiol-treated MCF-7 tumors, LV emboli, and LN metastases. Each triad was taken from the same mouse. Anti-rabbit CK18 and anti-mouse BrdUrd primary antibodies and goat anti-rabbit (*red*) and goat anti-mouse (*green*) antibodies were used. A DAPI counterstain (*blue*) was occasionally included. The centrally necrotic regions of tumors were excluded from analyses. *C,* quantification of *A* and *B* ($n = 5$ for tumors and LNs; $n = 3$ for LVs), showing the data obtained from the HRP based protocol in *A* (*white columns*) and the dual CK18/BrdUrd protocol in *B* (*black columns*).

16
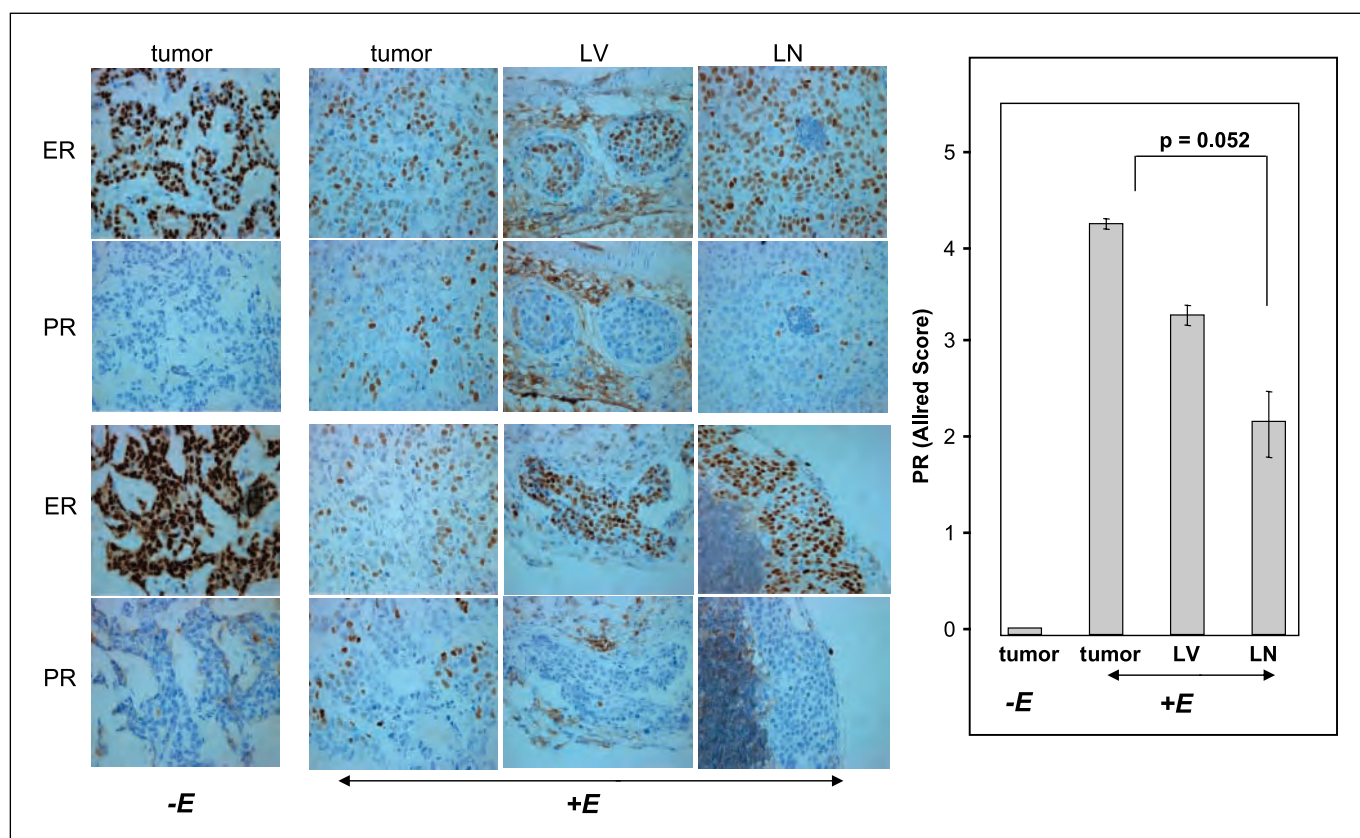
Figure 6. ER and PR expression in triads of MCF-7 tumors, LV emboli, and LN metastases. *Left,* representative images of two tumors from placebo ($-E$) treated mice and of two matched triads of estradiol-treated ($+E$) mice, showing tumors, their lymphatic emboli, and LN metastases. Paraffin-embedded sections were probed with mouse anti-ER or mouse anti-PR primary antibodies, coupled with goat anti-mouse HRP-conjugated secondary antibodies. *Right,* quantification of PR expression in placebo-treated ($n = 3$) and estradiol-treated tumors ($n = 7$), LV emboli ($n = 3$), and LN metastases ($n = 5$), based on the intensity of cellular staining combined with the percent of positive cells.

nonsignificant slight increase in ER expression in the LN metastases compared with the down-regulated ER in the estradiol-treated primary tumor.

Selection of cells for lymphatic transit: CD44. Hyaluronan regulates various aspects of cell behavior, particularly cell migration and invasiveness. It does so by binding to specific receptors on the cell surface, the best characterized of which is CD44 (22). Human breast cancer cells migrate directionally in response to a hyaluronan gradient depending on CD44 expression levels (22). Breast cancers secrete factors that up-regulate hyaluronan expression in osteoblasts (27), which may promote bone metastasis. Figure 7*A* shows CD44 expression levels in two primary tumors and in their LV and/or LN metastases. Set A (*top*) clearly shows extensive overexpression of CD44 in tumor cells occupying the LN microenvironment, compared with the same tumor cells in the mammary gland, where CD44 expression is sparse and heterogeneous. Set B includes a matched LV embolus and again shows sparse and heterogeneous CD44 in the tumor, but homogenous and elevated CD44 in both the LV embolic tumor cells, and the LN metastases.

Distant metastases. Metastases to distant organs were occasionally observed with these models. Figure 7*B* (*left*) shows H&E staining of tumor cells metastatic to the lung. Their identity is confirmed by intense ZsGreen fluorescence in a serial section (Fig. 7*B, right*). These lung metastases could have arisen by direct peritumoral venous invasion and spread (the most direct route to the lungs from distant body sites) or they may reflect indirect spread from an overwhelmed lymphatic system via lymphatic-venous anastomoses. Both mechanisms may contribute to distant organ metastasis in humans (28). It should be stressed that these metastases were rare and they occurred only in animals that also had extensive LN spread.

Perineurial invasion. Perineurial invasion was also noted in tumors arising from both cell lines. Perineurial invasion is observed in a variety of human carcinomas and may contribute to local-regional tumor spread, although it has not been shown to be an independent prognostic indicator in human mammary carcinomas (29). Although not as frequent as lymphatic invasion, perineurial invasion was occasionally found at tumor margins and along the peripheral nerves that parallel the iliac veins. Figure 7*C* shows an H&E stain (*left*) and CK18 immunohistochemistry (*right*) of T47D tumor cells (*arrow*) tracking along a peripheral nerve (*asterisk*).

Discussion

LN metastasis in association with tumor size is the single most powerful indicator of poor prognosis in mammary carcinoma (30, 31). Pathologic data sets of patients with breast cancer indicate that, at diagnosis, presence of tumor-infiltrated LNs is common, with estimates ranging from 30% to 50% of cases (32–34), depending on tumor size. The dominant feature of the present model is rapid and reliable LN metastasis of ER+ cells

17

from orthotopic tumor sites. Two different cell lines, MCF-7 and T47D, generated estrogen-dependent solid tumors and reliably produced metastases to local and distant LNs. Under conditions of the studies, which were terminated at 12 weeks, tumor cells in LV and LN metastases were observed in 75% of all mice and in essentially 100% of mice, the primary tumors of which exceeded ~ 75 mm^2 in area (Fig. 3). Clinically, the association between tumor size and LN involvement is well known (35). Metastases to other sites, like the lungs (Fig. 7B), were occasionally observed, as were cells migrating along peripheral nerve tracks (Fig. 7C). The ability of the latter routes to reliably colonize distant organs undoubtedly will require longer observation times. This is suggested by the studies of others. Half a million ER− MDA-231 breast cancer cells, injected directly into the circulation, nevertheless required 10 to 12 weeks before exhibiting limb bone metastases in 30% of mice (36). ER+ ZR75 cells injected into the circulation of mice required 3 to 6 months to yield similar bone metastases (37).
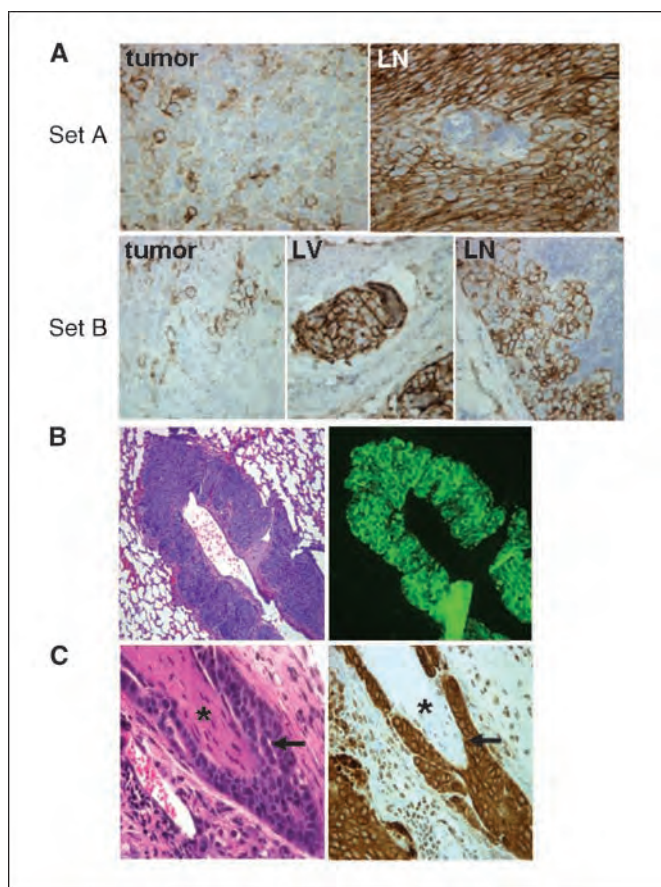
Use of modified breast cancer cells overexpressing hormones (38), growth factors (14, 39), and oncogenes (12) shows that the

Figure 7. Selection of CD44+ MCF-7 tumor cells for lymphatic transit and examples of lung metastases and perineurial invasion. *A,* tumors (*n* = 5) taken from estradiol-treated mice, and their matched LV (*n* = 3) and/or LNs (*n* = 6), were probed with mouse anti-CD44 and goat anti-mouse HRP-conjugated secondary antibodies. *Top,* a tumor and its matching LN. *Bottom,* a triad of tumor, LV, and LN taken from the same mouse. *B, left,* H&E stain of a paraffin-embedded section of T47D cells from an estradiol-treated mouse with metastasis to the lung. *Right,* a serial section processed for fluorescence microscopy. *C, left,* H&E stain of MCF-7 tumor cells from an estradiol-treated mouse showing perineurial invasion. *Right,* CK18 stain of a deeper section. *, nerve; *arrow,* tumor cells.

metastatic potential, route of dispersal, time to metastasis, and preferred organ arrest site of any cell line are dependent on unique factors elaborated by that cell, and that much remains to be learned about the role of estrogens and progestins on these processes. For example, it has been reported that clinically, ER+ tumors are more likely to spread to bones whereas ER− tumors more commonly metastasize to the viscera (40, 41). ER+ metastasis models, reflecting the clinical situation, could help define molecular mechanisms involved in such tissue specificity.

Expression profiling of matched primary and metastatic LN tumor pairs in clinical samples has failed to identify genes that distinguish one from the other (42) because metastases are genetically more closely related to the primary tumor from which they arose than to any other metastasis. However, within matched pairs, select genes are differentially expressed between the tumor and LN metastasis. Common among these are extracellular matrix and cell-matrix interacting genes, like the hyaluronan receptor CD44, which mediates rolling, attachment, and migration of cells on a hyaluronan substratum (43, 44). We show here that CD44 is sparsely and heterogeneously expressed in primary tumors but homogeneously overexpressed in LV tumor cell emboli and LN metastases (Fig. 7). Because directional migration of breast cancer cells towards hyaluronan is dependent on CD44 (22), we propose that the CD44+ subpopulation of primary tumor cells is preferentially propelled into tumoral lymphatics, and from there to LNs. If so, therapeutic targeting of the CD44+ subpopulation in a primary tumor could prevent LN metastases.

There is a high concordance rate (~80-90%) in ER expression between primary tumors and matched LN metastases (5). However, in the same patient, considerable disparities can exist in the concentrations of ER at the two sites, with ER levels often (6, 45) but not always (45) higher in the LN than in the local primary tumor. We observe a pattern (Fig. 6) in which ER levels are higher in the LN than in the primary tumor of the same mouse, an indicator of ER down-regulation failure in the LN microenvironment. It has been reported that there is an association between estrogen-dependent ER down-regulation and improved transcriptional efficacy of the receptors (46). Although it might be counterintuitive to think that in the presence of estrogen, lower ER levels signal a stronger hormone response, this seems to be the case. Thus, the inefficient ER down-regulation in the LN could be associated with poorer hormone responsiveness at that site. In the mouse tumors, PR expression levels (Fig. 6), which are markers of estrogen action and ER function, support this hypothesis. Assessment of PR levels in LNs and matched primary tumors shows a trend towards a decrease in LN PR (Fig. 6). This would be predicted by inefficient ER down-regulation. Clinically, both up-regulation and down-regulation of PR have been reported in the LN compared with primary tumors (45), but this has not been correlated to ER in the same samples.

We also observe a statistically significant increase in the proliferation rate of LN metastases compared with matched primary tumors (Fig. 5B and C). Clinically, increased mitoses in nodal metastases compared with primary tumors have been reported (47), possibly due to release of cytokines and growth factors, such as insulin-like growth factor-I and epidermal growth factor, by the LN (48). The implications of this growth promotion within LNs for failure of hormone treatments in metastatic disease could be important. If, in the LN microenvironment, cytokines and growth factors are the dominant mitogens, then LN metastases would be less sensitive than primary tumors to estradiol-suppressive therapies. Indeed, in metastatic disease,

tamoxifen, which targets ER signaling pathways, is rarely associated with long-term remission, exhibiting decreased mean time to disease progression and decreased duration of response than local disease (41, 49, 50).

In summary, we have developed models of ER+ human breast cancers that reliably spread to LNs from solid tumors. Through the use of a new generation fluorescent protein, ZsGreen, we are able to identify cancer cells in tumors, LV emboli, LNs, and, occasionally, more distant sites for further molecular analysis. These studies show that the tumor cells found in LNs overexpress markers associated with tumor aggressiveness. At the same time, the LN microenvironment may suppress estrogen sensitivity of tumor cells, which would make them more resistant than primary tumors to ER-targeted treatments.

References

1. Hayes DF, Isaacs C, Stearns V. Prognostic factors in breast cancer: current and new predictors of metastasis. J Mammary Gland Biol Neoplasia 2001;6:375–92.
2. Parkin DM, Bray F, Ferlay J, Pisani P. Global cancer statistics, 2002. CA Cancer J Clin 2005;55:74–108.
3. Keen JC, Davidson NE. The biology of breast carcinoma. Cancer 2003;97:825–33.
4. Zheng WQ, Lu J, Zheng JM, Hu FX, Ni CR. Variation of ER status between primary and metastatic breast cancer and relationship to p53 expression. Steroids 2001;66:905–10.
5. Butler JA, Trezona T, Vargas H, State D. Value of measuring hormone receptor levels of regional metastatic carcinoma of the breast. Arch Surg 1989;124:1131–4; discussion 4–5.
6. Hoehn JL, Plotka ED, Dickson KB. Comparison of estrogen receptor levels in primary and regional metastatic carcinoma of the breast. Ann Surg 1979;190:69–71.
7. Clarke R. Human breast cancer cell line xenografts as models of breast cancer. The immunobiologies of recipient mice and the characteristics of several tumorigenic cell lines. Breast Cancer Res Treat 1996;39:69–86.
8. Osborne CK, Hobbs K, Clark GM. Effect of estrogens and antiestrogens on growth of human breast cancer cells in athymic nude mice. Cancer Res 1985;45:584–90.
9. Lacroix M, Leclercq G. Relevance of breast cancer cell lines as models for breast tumours: an update. Breast Cancer Res Treat 2004;83:249–89.
10. Mukhopadhyay R, Theriault RL, Price JE. Increased levels of α6 integrins are associated with the metastatic phenotype of human breast cancer cells. Clin Exp Metastasis 1999;17:325–32.
11. Yoneda T, Williams PJ, Hiraga T, Niewolna M, Nishimura R. A bone-seeking clone exhibits different biological properties from the MDA-MB-231 parental human breast cancer cells and a brain-seeking clone *in vivo* and *in vitro*. J Bone Miner Res 2001;16:1486–95.
12. Dickson RB, Kasid A, Huff KK, et al. Activation of growth factor secretion in tumorigenic states of breast cancer induced by 17 β-estradiol or v-Ha-ras oncogene. Proc Natl Acad Sci U S A 1987;84:837–41.
13. Benz CC, Scott GK, Sarup JC, et al. Estrogen-dependent, tamoxifen-resistant tumorigenic growth of MCF-7 cells transfected with HER2/neu. Breast Cancer Res Treat 1993;24:85–95.
14. Mattila MM, Ruohola JK, Karpanen T, Jackson DG, Alitalo K, Harkonen PL. VEGF-C induced lymphangiogenesis is associated with lymph node metastasis in orthotopic MCF-7 tumors. Int J Cancer 2002;98:946–51.
15. McLeskey SW, Zhang L, Kharbanda S, et al. Fibroblast growth factor overexpressing breast carcinoma cells as models of angiogenesis and metastasis. Breast Cancer Res Treat 1996;39:103–17.
16. Lin CQ, Singh J, Murata K, et al. A role for Id-1 in the aggressive phenotype and steroid hormone response of human breast cancer cells. Cancer Res 2000;60:1332–40.
17. Belguise K, Kersual N, Galtier F, Chalbos D. FRA-1 expression level regulates proliferation and invasiveness of breast cancer cells. Oncogene 2005;24:1434–44.

18. Thompson EW, Brunner N, Torri J, et al. The invasive and metastatic properties of hormone-independent but hormone-responsive variants of MCF-7 human breast cancer cells. Clin Exp Metastasis 1993;11:15–26.
19. Hoffman RM. The multiple uses of fluorescent proteins to visualize cancer *in vivo*. Nat Rev Cancer 2005;5:796–806.
20. Kim LS, Huang S, Lu W, Lev DC, Price JE. Vascular endothelial growth factor expression promotes the growth of breast cancer brain metastases in nude mice. Clin Exp Metastasis 2004;21:107–18.
21. Richards B, Zharkikh L, Hsu F, Dunn C, Kamb A, Teng DH. Stable expression of Anthozoa fluorescent proteins in mammalian cells. Cytometry 2002;48:106–12.
22. Tzircotis G, Thorne RF, Isacke CM. Chemotaxis towards hyaluronan is dependent on CD44 expression and modulated by cell type variation in CD44-hyaluronan binding. J Cell Sci 2005;118:5119–28.
23. Sartorius CA, Groshong SD, Miller LA, et al. New T47D breast cancer cell lines for the independent study of progesterone B- and A-receptors: only antiprogestin-occupied B-receptors are switched to transcriptional agonists by cAMP. Cancer Res 1994;54:3868–77.
24. Sartorius CA, Shen T, Horwitz KB. Progesterone receptors A and B differentially affect the growth of estrogen-dependent human breast tumor xenografts. Breast Cancer Res Treat 2003;79:287–99.
25. Harvey JM, Clark GM, Osborne CK, Allred DC. Estrogen receptor status by immunohistochemistry is superior to the ligand-binding assay for predicting response to adjuvant endocrine therapy in breast cancer. J Clin Oncol 1999;17:1474–81.
26. Shafie SM, Grantham FH. Role of hormones in the growth and regression of human breast cancer cells (MCF-7) transplanted into athymic nude mice. J Natl Cancer Inst 1981;67:51–6.
27. Bose N, Masellis AM. Secretory products of breast cancer cells up-regulate hyaluronan production in a human osteoblast cell line. Clin Exp Metastasis. In press 2006.
28. Kuman V, Fausto N, Abbas A, editors. Robbins and Cotran pathologic basis of disease. 7th ed. Philadelphia: Elsevier; 2004.
29. Mills SE, Carter D, Greenson JK, Oberman HA, Reuter V, Stoler MH, editors. Sternberg's diagnostic surgical pathology. 4th ed. Philadelphia: Lippincott, Williams and Wilkins; 2003.
30. McGuire WL. Prognostic factors for recurrence and survival in human breast cancer. Breast Cancer Res Treat 1987;10:5–9.
31. Foster RS, Jr. The biologic and clinical significance of lymphatic metastases in breast cancer. Surg Oncol Clin N Am 1996;5:79–104.
32. Vinh-Hung V, Verschraegen C, Promish DI, et al. Ratios of involved nodes in early breast cancer. Breast Cancer Res 2004;6:R680–8.
33. Veronesi U, Paganelli G, Viale G, et al. Sentinel lymph node biopsy and axillary dissection in breast cancer: results in a large series. J Natl Cancer Inst 1999;91:368–73.
34. Jatoi I, Hilsenbeck SG, Clark GM, Osborne CK. Significance of axillary lymph node metasta-

sis in primary breast cancer. J Clin Oncol 1999;17:2334–40.
35. Carter CL, Allen C, Henson DE. Relation of tumor size, lymph node status, and survival in 24,740 breast cancer cases. Cancer 1989;63:181–7.
36. Kang Y, Siegel PM, Shu W, et al. A multigenic program mediating breast cancer metastasis to bone. Cancer Cell 2003;3:537–49.
37. Guise TA, Yin JJ, Mohammad KS. Role of endothelin-1 in osteoblastic bone metastases. Cancer 2003;97:779–84.
38. Guise TA, Yin JJ, Thomas RJ, Dallas M, Cui Y, Gillespie MT. Parathyroid hormone-related protein (PTHrP)-(1-139) isoform is efficiently secreted *in vitro* and enhances breast cancer metastasis to bone *in vivo*. Bone 2002;30:670–6.
39. Padera TP, Kadambi A, di Tomaso E, et al. Lymphatic metastasis in the absence of functional intratumor lymphatics. Science 2002;296:1883–6.
40. Koenders PG, Beex LV, Langens R, Kloppenborg PW, Smals AG, Benraad TJ. Steroid hormone receptor activity of primary human breast cancer and pattern of first metastasis. The Breast Cancer Study Group. Breast Cancer Res Treat 1991;18:27–32.
41. Fuqua SA. The role of estrogen receptors in breast cancer metastasis. J Mammary Gland Biol Neoplasia 2001;6:407–17.
42. Weigelt B, Wessels LF, Bosma AJ, et al. No common denominator for breast cancer lymph node metastasis. Br J Cancer 2005;93:924–32.
43. Toole BP. Hyaluronan: from extracellular glue to pericellular cue. Nat Rev Cancer 2004;4:528–39.
44. Clark RA, Alon R, Springer TA. CD44 and hyaluronan-dependent rolling interactions of lymphocytes on tonsillar stroma. J Cell Biol 1996;134:1075–87.
45. De la Haba-Rodriguez JR, Ruiz Borrego M, Gomez Espana A, et al. Comparative study of the immuno-histochemical phenotype in breast cancer and its lymph node metastatic location. Cancer Invest 2004;22:219–24.
46. Lonard DM, Nawaz Z, Smith CL, O'Malley BW. The 26S proteasome is required for estrogen receptor-α and coactivator turnover and for efficient estrogen receptor-α transactivation. Mol Cell 2000;5:939–48.
47. Hasebe T, Konishi M, Iwasaki M, et al. Histological characteristics of tumor cells and stromal cells in vessels and lymph nodes are important prognostic parameters of extrahepatic bile duct carcinoma: a prospective study. Hum Pathol 2005;36:655–64.
48. LeBedis C, Chen K, Fallavollita L, Boutros T, Brodt P. Peripheral lymph node stromal cells can promote growth and tumorigenicity of breast carcinoma cells through the release of IGF-I and EGF. Int J Cancer 2002;100:2–8.
49. Rose C, Mouridsen HT. Treatment of advanced breast cancer with tamoxifen. Recent Results Cancer Res 1984;91:230–42.
50. Bratherton DG, Brown CH, Buchanan R, et al. A comparison of two doses of tamoxifen (Nolvadex) in postmenopausal women with advanced breast cancer: 10 mg bd versus 20 mg bd. Br J Cancer 1984;50:199–205.

Tissue-Engineered Bone Is a Breast Cancer Target

Moreau *et al.* _____ **Page 10304**

The high propensity of breast cancer to metastasize to bone results from contributions on both sides of the tumor-stroma interface. Identifying the components in bone (growth factors, etc.) essential for metastasis is challenging. To investigate bone–breast cancer interactions, Moreau and colleagues created engineered bone by adding human marrow-derived mesenchymal stem cells to silk fiber scaffolds. Later, metastases were demonstrated to form in engineered bone from human breast cancer cells originating at the orthotopic site in a mouse model. Since engineered bone can be manipulated in controlled fashion, it is now possible to use it to identify bone components essential for metastasis.

Pregnane X Receptor Enhances Chemotherapy in Prostate Cancer

Chen *et al.* _____ **Page 10361**

As a sensor of xenobiotics, pregnane X receptor (PXR) regulates the gene expression of drug metabolizing enzymes and efflux transporters that can have profound effects on the efficacy of chemotherapy. Chen and colleagues found that prostate cancer cells expressed functional PXR which, when activated, rendered tumor cells with increased resistance to Taxol and vinblastine. Ablation of PXR in prostate cancer cells enhanced the efficacy of chemotherapy. Since PXR can be activated by a range of chemotherapeutics and herbal supplements, potential activation of PXR should be taken into consideration when designing combination chemotherapy for prostate cancer.

Mutagenesis Screen Indentifies EGFR Inhibitors

Yu *et al.* _____ **Page 10417**
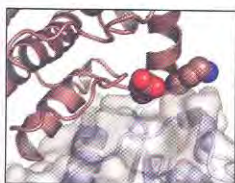
Secondary EGFR mutations commonly lead to resistance to the EGFR inhibitors erlotinib and gefitinib in patients with non–small cell lung cancer. Irreversible EGFR inhibitors, such as CL-387,785 can overcome resistance and are in clinical development. Yu and colleagues developed a cell-based, *in vitro* random mutagenesis screen to identify EGFR mutations that confer resistance to CL-387,785 and identified a number of novel resistance mutations. Both an alternative EGFR inhibitor and a Cdk4 inhibitor could overcome such resistance. These results identify novel mutations mediating resistance to irreversible EGFR inhibitors and reveal alternative strategies to overcome or prevent resistance in EGFR-mutant lung cancers.

Aromatase Levels Predict Survival in Women with Lung Cancer

Mah *et al.* _____ **Page 10484**
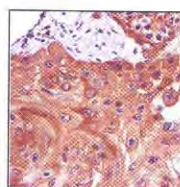
Lung cancer remains the most lethal type of human malignancy, with increased incidences occurring especially in women. Mah and coauthors describe novel findings about the prognostic value of aromatase expression in predicting the course of non–small cell lung cancer (NSCLC). This group demonstrated the importance of estrogen and aromatase for promoting tumor progression in a mouse model. They further conducted a population-based study examining aromatase levels in human NSCLC using tissue microarray technology. Lower levels of aromatase were a strong predictor of survival in women older than 65 years with earlier stage cancer. The authors predict that the use of aromatase inhibitors may benefit this patient population.

Lymph Node Microenvironment Alters Sensitivity to Estradiol

Harrell *et al.* _____ **Page 10582**

Estrogen-responsive breast tumors often become refractory to antiestrogens and recur in organs distant from the primary site. To determine if the lymph node (LN) microenvironment alters tumor-cell sensitivity to estradiol, Harrell and colleagues developed a model to assess the hormone responsiveness of xenografted human breast tumors and their matched LN metastases. Laser-capture microdissection plus gene expression profiling confirmed by immunohistochemistry, found that LN metastases were estrogen insensitive compared to the primary tumors. Indeed, some genes were regulated by estradiol in the opposite direction in tumors and matched metastases. This study shows that the LN microenvironment influences expression of therapeutic targets that may alter cancer cell survival, recurrence, or response to treatments.

Estrogen Insensitivity in a Model of Estrogen Receptor–Positive Breast Cancer Lymph Node Metastasis

Joshua Chuck Harrell,[1,3] Wendy W. Dye,[1] Djuana M.E. Harvell,[1] Mauricio Pinto,[1] Paul Jedlicka,[2] Carol A. Sartorius,[1] and Kathryn B. Horwitz[1,2,3]

[1]Division of Endocrinology, Department of Medicine, [2]Department of Pathology, and [3]Program in Reproductive Sciences, University of Colorado Health Sciences Center, Aurora, Colorado

Abstract

The lymphatic system is a common avenue for the spread of breast cancer cells and dissemination through it occurs at least as frequently as hematogenous metastasis. Approximately 75% of primary breast cancers are estrogen receptor (ER) positive and the majority of these maintain receptor expression as lymph node (LN) metastases. However, it is unknown if ER function is equivalent in cancer cells growing in the breast and in the LNs. We have developed a model to assess estrogen responsiveness in ER+ breast tumors and LN metastases. Fluorescent ER+ MCF-7 tumors were grown in ovariectomized nude mice supplemented with estradiol. Once axillary LN metastasis arose, estradiol was withdrawn (EWD), for 1 or 4 weeks, or continued, to assess estradiol responsiveness. On EWD, proliferation rates fell similarly in tumors and LN metastases. However, estradiol-dependent ER down-regulation and progesterone receptor induction were deficient in LN metastases, indicating that ER-dependent transcriptional function was altered in the LN. Cancer cells from estradiol-treated and EWD primary tumors and matched LN metastases were isolated by laser capture microdissection. Global gene expression profiling identified transcripts that were regulated by the tissue microenvironment, by hormones, or by both. Interestingly, numerous genes that were estradiol regulated in tumors lost estradiol sensitivity or were regulated in the opposite direction by estradiol in LN metastases. We propose that the LN microenvironment alters estradiol signaling and may contribute to local antiestrogen resistance. [Cancer Res 2007;67(21):10582–91]

Introduction

Interactions between luminal epithelial cells and the surrounding microenvironment govern the overall physiology of the mammary gland (1), with development of epithelial ducts being dependent on the activity of both stromal and epithelial estrogen receptor α (ERα; ref. 2). Integrins, growth factors, and steroid hormone signaling pathways all play an important part in maintaining normal glandular architecture (3). Stroma makes up >80% of breast volume and is composed of fat, interstitial/interlobular dense connective tissue, intralobular loose connective tissue, and lymphatic/blood vessels (4). Luminal epithelial cells associate with these stromal elements as well as with basement membrane and myoepithelial cells. Disruption of this delicate balance results in dramatic changes in both extracellular and intracellular signaling (3).

Seventy percent to 80% of primary breast tumors express ERα and initially respond to estradiol withdrawal (EWD) or antiestrogen therapies (5). Breast cancer ERα expression and function are also influenced by the cellular microenvironment. *In vitro* studies with human ER+ breast cancer cells show that extracellular matrix proteins, such as type I collagen and laminin, can modify proliferative responsiveness to estrogen (6). A comparison of *in vitro* and *in vivo* models found that estradiol regulates different genes in human breast tumor xenografts compared with the identical cells in culture (7). These studies suggest that a microenvironment-dependent influence on estradiol-dependent gene expression exists in ER+ breast cancers. However, this issue has received little attention, and to the best of our knowledge, *in vivo* experiments that test if metastatic microenvironments alter estradiol-dependent gene expression have not been conducted.

Metastasis to the lymph nodes (LN) is a key prognostic factor that conveys advanced disease status with the possibility that cancer cells have spread to other more distant sites. At diagnosis, 30% to 50% of all breast cancers have spread to the draining or "sentinel" LN (8–10), and if the primary tumor is ER+, then ∼80% of LN metastases retain ER expression (11–13). As tumor cells disseminate to LNs, they enter a distinct microenvironment. Here, they encounter different supporting elements, such as reticular fibers, flowing lymph fluid, lymphocytes, T and B cells, increased numbers of macrophages, and epithelial reticular cells that are surrounded by adipose tissue (14). It is unknown if the differences in structure, function, and composition of the mammary gland compared with the LN affect ER activities and estradiol-dependent gene expression in breast cancer cells that are located within these two distinct microenvironments.

The studies presented here use a xenograft model of fluorescent, ER+, estradiol-dependent human breast cancer LN metastasis to address this question. In the same mouse, LN metastases are found to be transcriptionally estradiol insensitive compared with primary tumors from which they originated, despite retention of ER. We identify genes that may aid in explaining mechanistically why advanced ER+ breast cancers become nonresponsive to antiestrogen or EWD therapies and often recur as metastases.

Materials and Methods

Cell lines. MCF-7 human breast cancer cells were originally purchased from the American Type Culture Collection. The generation of fluorescent MCF-7 cells has been previously described (15). In brief, ZsGreen retroviral particles (Clontech) were isolated from PT-67 packaging cells (Clontech), filtered, and overlaid onto MCF-7 cells. Cells were serially transduced twice for 24 h each round and then subjected to G418 selection followed by aseptic fluorescence-associated cell sorting to isolate a homogeneously

bright green subpopulation. Generation of PR-B–expressing T47D human breast cancer cells has been described previously (16).

Xenograft tumor growth and metastases. All animal procedures were done under a protocol approved by the University of Colorado Institutional Animal Care and Use Committee. Ovariectomized female athymic *nu/nu* mice were obtained from Harlan Sprague Dawley at 5 to 6 weeks of age. To establish tumors, animals were anesthetized with Avertin and injected into the opening of the lactiferous duct of abdominal mammary glands with 1 million ZsGreen-expressing MCF-7 cells in 100 µL of 100% Matrigel (Becton Dickinson). Mice were also implanted with silastic pellets containing 17β-estradiol (2 mg + 8 mg cellulose) as previously described (17). Fluorescent whole-body imaging (Illumatool 9900, Lightools Research) was done weekly to determine when axillary LN metastases arose. For EWD mice, once axillary LN metastases were detected, mice were anesthetized with Avertin and estradiol-releasing pellets were removed for 1 week; some were removed for 4 weeks to confirm protein expression and for proliferation studies. Control mice were continued on estradiol. Mice were euthanized by CO_2 asphyxiation and fluorescent intravital optical imaging was done by coupling the Illumatool with an Olympus SZ-61 dissecting microscope and Olympus C-5050 digital camera. Fluorescent tumors in mammary glands and LNs were removed. Lymphatic vessels (LV) draining fluorescent tumor cells from mammary glands were also collected.

Serial passaging of a ZsGreen⁺ T47D-PR-B LN metastasis was done by isolating the LN, pushing the tissue through multiple sieves, expanding and G418 selecting human tumor cells in culture, and reinjecting the cells into the mammary glands of estradiol-supplemented recipient mice.

Laser capture microdissection and expression profiling. Mammary gland tumors (MGT) and LN metastases from estradiol-treated or 1-week EWD mice were harvested, placed in a Tissue-Tek cryomold (EMS), covered with Neg50 frozen section medium (Richard-Allan Scientific), and frozen in isopentane (Sigma) cooled by liquid nitrogen. Sections (8 µm) were cut through the entire tissue with a cryotome set at $-20°C$. Each section was collected on an uncharged slide (Fisher), and every 10th slide was stained for H&E or processed for cytokeratin 18 (CK18) immunofluorescence. Slides containing cancer cells were processed through 75% ethanol, water, 75% ethanol, 95% ethanol, and 100% ethanol for 30 s each and finally dehydrated with xylene for 1 min before being immediately subjected to laser capture microdissection using an Arcturus Autopix. Two thousand cells for each sample were extracted within 30 min of fixation and frozen at $-70°C$ until further processing. Suggested protocols from Arcturus were followed for RNA extraction and two rounds of amplification using the PicoPure RNA isolation kit and RiboAmp HS kit (Arcturus), respectively. Samples were *in vitro* transcribed, biotinylated, hybridized to Affymetrix X3P chips that interrogate 47,000 transcripts with 61,000 probe sets, and scanned on an Agilent Bioanalyzer 2100.

Statistical analyses. Raw expression values for each tumor and LN were downloaded into GeneSpring version 7.3 (Agilent) for exploratory purposes. Four matched pairs of tumors and metastatic LNs (2 estradiol and 2 EWD) as well as 2 unmatched LNs (1 estradiol and 1 EWD) for a total of 10 samples were analyzed. Probe sets that were absent across all 10 samples were filtered from further statistical analysis (18). Remaining probe sets were robust multiarray analysis (RMA) normalized in Partek Genomics Suite 6.2, and a three-way mixed model ANOVA analysis was done to identify differentially expressed genes. Four groups were compared: estradiol-treated MGT, estradiol-treated LN, EWD MGT, and EWD LN. These four groups were divided based on the two levels of hormone treatment (estradiol or EWD) and the two levels of tissue type (MGT or LN). Hormone and tissue were therefore defined as main factors in the model. Interaction effects among hormone and tissue were also included. The random factor animal (which is nested in hormone) was added to account for the fact that multiple tissues (MGT and LN) were taken from the same animal. In total, 1,570 transcripts were identified as having significant differences among the four group means ($P_{model} < 0.05$) and $P < 0.05$ for main or interaction effects. To further identify differences in hormonal regulation among the 1,570 differentially expressed genes, they were subjected to linear contrasts to make two specific comparisons: EWD versus estradiol-treated MGT and EWD versus estradiol-treated LN. Bonferroni's correction for multiple tests was then applied to these two comparisons and the level of significance was changed to 0.025.

Gene networking. To define relationships among genes differentially regulated by estradiol in MGTs and LN metastases, pathway analyses were done using Ingenuity software. Probe set identification numbers were used for gene identification.

Immunohistochemistry. Organs were fixed in 4% paraformaldehyde overnight, paraffin embedded, and cut into 4-µm sections. After high-temperature antigen retrieval in citrate buffer, immunohistochemistries were done on estradiol-treated tissues and 1-week or 4-week EWD mice using primary antibodies directed against ER (1:100, SP1; Lab Vision/NeoMarkers), progesterone receptor (PR; 1:500, 1294; Dako), CK18 (1:200; Calbiochem), CD44 (1:200; Ab4; Lab Vision/NeoMarkers), caveolin 1 (CAV1; 1:125; Epitomics), and cathepsin D (CTSD; 1:125; Epitomics) for 1 h at room temperature. Bound primary antibodies were detected with horseradish peroxidase (HRP)–conjugated goat anti-mouse and/or goat anti-rabbit secondary antibodies (Envision HRP; Dako) reacted with 3,3′-diaminobenzidine (Dako). Sections were counterstained with hematoxylin and mounted with Permount (Fisher). For immunofluorescence microscopy, goat anti-rabbit Alexa Fluor 555 (red) secondary antibodies were used (1:200, Alexa Fluors; Invitrogen) and sections were counterstained with 4′,6-diamidino-2-phenylindole (DAPI) in methanol and mounted with Gel/Mount (Biomeda).

Results

EWD model. MCF-7+ZsGreen tumors require estradiol for growth and LN metastasis (15). To generate LN metastases, bilateral tumors were grown in the abdominal mammary glands of ovariectomized immunocompromised mice that were supplemented with an estradiol-releasing pellet (Fig. 1*A*). Weekly tumor measurements were recorded with a digital caliper. Spread of cancer cells to axillary LNs was determined by weekly fluorescent whole-body imaging (Fig. 1*B*). To define estradiol-regulated genes (7), once LN metastases were detected, the estradiol-releasing pellet was withdrawn for 1 week in half of the mice (EWD) or left in place in the remaining mice. To assess proliferation rate, EWD was extended for 4 weeks in tumors and LN metastases. Bromodeoxyuridine labeling and mitotic indices indicated a similar decrease of ~50% at both sites. At necropsy, assessment of the uterine mass confirmed the presence or absence of systemic estradiol, with 1- and 4-week EWD uteri exhibiting significant decreases in mass compared with estradiol-treated uteri. To locate cancer cells within LNs, the entire LN was sectioned and every 10th slide was processed for CK18 immunohistochemistry (Fig. 1*C*). The CK18 map and the unique morphology of MCF-7 cells compared with lymphocytes (Fig. 1*D*) allowed for identification of the cancer cells in serial sections. We then marked and laser captured pure MCF-7 cell populations from matched tumors and LN metastases.

Estrogen insensitivity in LN metastases: ER and PR expression. Estradiol treatment leads to down-regulation of ER protein levels in tumors (19, 20). To characterize these effects in estradiol-free, estradiol-treated, and EWD conditions, the MCF-7 tumors, LV emboli, and LN metastases were probed for ER and PR by immunohistochemistry. In Fig. 2, the tissues from each treatment group were from the same mouse. Highest ER levels were present in tumors that did not receive supplemental estradiol (−E). Seventy-three percent of MCF-7 cells expressed high levels of ER and no cells contained PR (Fig. 2, *top*). In the presence of estradiol (+E), ERs were down-regulated by >40% in the tumor (Fig. 2, *middle*) but decreased by <20% in LV tumor emboli and LN metastasis of the same mouse. Ligand-dependent down-regulation of ER is required for its transcriptional activity (20), including PR
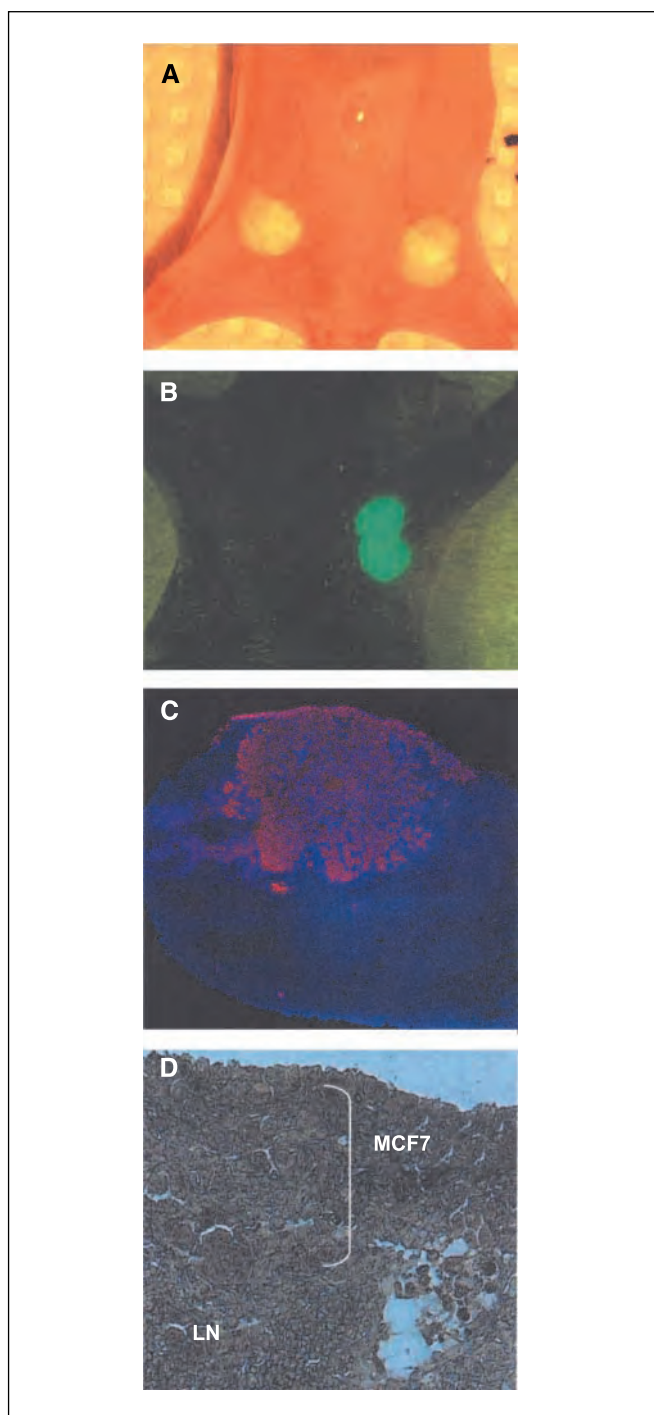
Figure 1. MCF-7+ZsGreen xenograft tumors and LN metastases. MCF-7+ZsGreen tumors were established in mammary glands of ovariectomized *nu/nu* mice supplemented with an estradiol pellet, and LN metastases were allowed to develop. *A,* fluorescent whole-body image of bilateral MCF-7+ZsGreen tumors. *B,* fluorescent whole-body image of MCF-7+ZsGreen metastasis to the left axillary LN. *C,* fluorescence immunohistochemistry for CK18 (*red*) and DAPI (*blue*) of an axillary LN metastasis. Magnification, ×4. *D,* white light laser capture microscope image of an axillary LN metastasis showing MCF-7 cells or lymphocytes (LN). Magnification, ×40.

induction. Indeed, PRs were expressed in +E tumors but were only rarely found in +E LV emboli (Fig. 2, *arrows*) or in LN metastases. On EWD, ERs were restored to control (−E) levels in all tissues, and PRs were absent (Fig. 2, *bottom*).

Microenvironment versus clonal selection. To determine whether the increased ER expression observed in LN metastases was due to clonal selection of ER^{+} cells from the primary tumor, or to an effect on ER at the metastatic microenvironment, tumor cells were isolated from the axillary LN metastasis of a donor mouse, expanded in culture, and reimplanted in the mammary gland of an
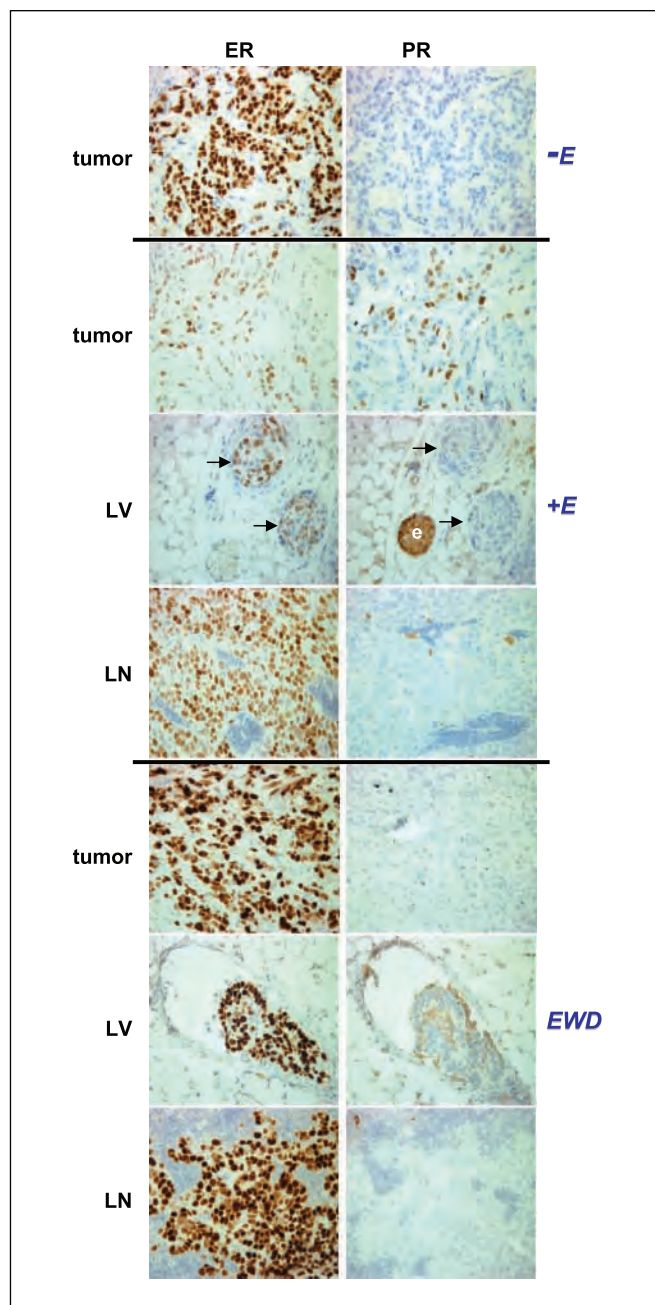
Figure 2. Estradiol regulation of ER and PR levels. ER and PR expression in MCF-7 cells from matched tumors, LVs, and LNs. MCF-7+ZsGreen tumors were established in ovariectomized mice supplemented with a placebo pellet (−E), an estradiol-releasing pellet (+E), or an estradiol-releasing pellet until LN metastases arose, after which the estradiol pellet was withdrawn for 1 wk (*EWD*). The primary tumors, efferent LVs, and draining LNs from the same mouse were dissected and prepared for histology. Paraffin-embedded sections were probed with rabbit anti-ER or mouse anti-PR primary antibodies coupled with goat anti-rabbit (ER) or goat anti-mouse (PR) HRP-conjugated secondary antibodies. Background staining of erythrocytes (*e*). *Arrows* point to the LV.

23

Figure 3. Aberrant ER regulation in tumor cells located in the LN microenvironment and global gene expression profiling of tumors and matched LN metastases. *A,* ER immunohistochemistry of estradiol-treated T47D tumors and their matched LN metastases. An estradiol-treated MGT in mouse 1 developed LN metastases. Cells from the LN metastasis of mouse 1 were expanded in culture and reinjected into the mammary gland of a second estradiol-treated recipient mouse 2, which also yielded LN metastases. MGTs and LN metastases from both mice were paraffin embedded, sectioned, and stained for ER by immunohistochemistry. *B,* unsupervised hierarchical clustering from continuously estradiol-treated (+*E*) or 1-wk EWD tumors and matched LN metastases. *Red,* up-regulated transcripts; *blue,* down-regulated transcripts; *gray,* relatively unchanged transcripts. *C,* ANOVA analysis identified 1,570 genes with tissue effects, hormone effects, and/or interaction effects.
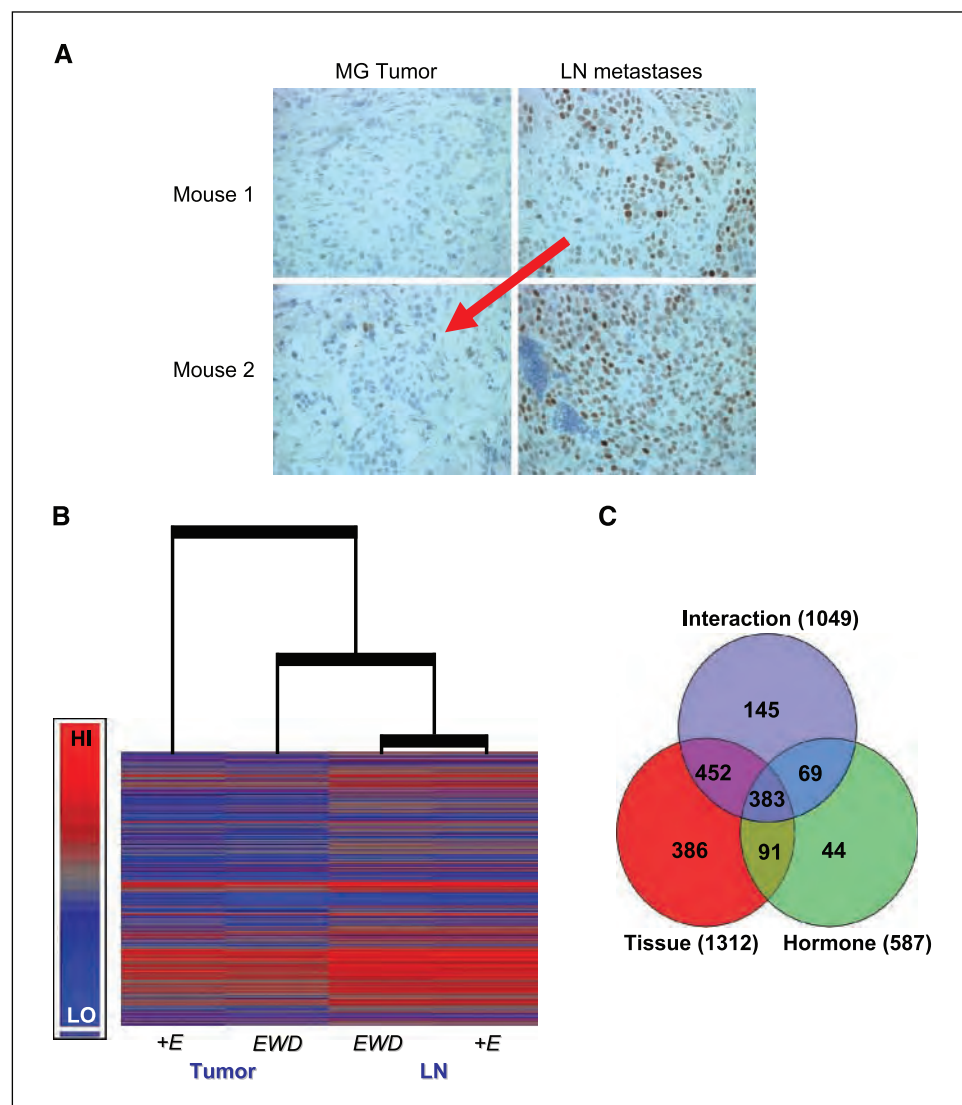
estradiol-treated recipient mouse. This tumor also yielded a LN metastasis. Figure 3*A* (*top*) shows ER immunohistochemistry of the estradiol-treated primary MGT and its matched LN metastasis from the donor mouse (mouse 1). ERs in the tumor grown in the mammary gland and LN of the recipient mouse (mouse 2) are shown in Fig. 3*A* (*bottom*). There was a 2-fold increase in ER content in the cancer cells populating the LN of mouse 1 and a similar 2-fold increase in the LN ER of mouse 2. These data suggest that the LN microenvironment rather than clonal selection modifies ER expression levels in response to estradiol.

Global gene expression profiling. To determine if the apparent estradiol insensitivity of LN metastases as assessed by ER down-regulation and failure of PR induction extends to other estradiol-dependent genes, global gene expression profiling was done. To ensure that only human tumor cells were evaluated, pure cell populations were isolated by laser capture microdissection. Estradiol-treated and 1-week EWD tumors and their matched LN metastases were analyzed to define the subset of estradiol-regulated genes (7). Unsupervised hierarchical clustering showed that EWD had a lesser effect on genes in LN metastases than on genes in MGTs, with the estradiol-treated and EWD LN metastases clustering closest

together (Fig. 3*B*). Interestingly, the EWD tumors clustered closer to the LNs than to the estradiol-treated tumors.

To identify genes with differential expression patterns, a three-way mixed model ANOVA was done for genes that were present in at least one condition. Genes with the greatest differences in expression due to the hormone treatment, tissue type, interaction between hormone and tissue, or within and between animals ($P_{model} < 0.05$) and with significant ($P < 0.05$) main (tissue and/or hormone effects) or interaction effects were sorted to yield a total of 1,570 differentially expressed transcripts. Significant main effects indicate simple differences between the two hormone and/or two tissue groups, an example being that all EWD tissues have higher gene expression levels than all estradiol-treated tissues (regardless of tissue type) or that all LN tissues have higher gene expression levels than all MGT (regardless of hormone treatment). Significant interaction effects, on the other hand, indicate complex differences in which the results of one factor differ depending on the levels of the other factor. For example, a gene that was expressed at higher levels in estradiol-treated LNs than MGTs but in EWD tissues had the opposite pattern with higher levels in MGTs than LNs.

24
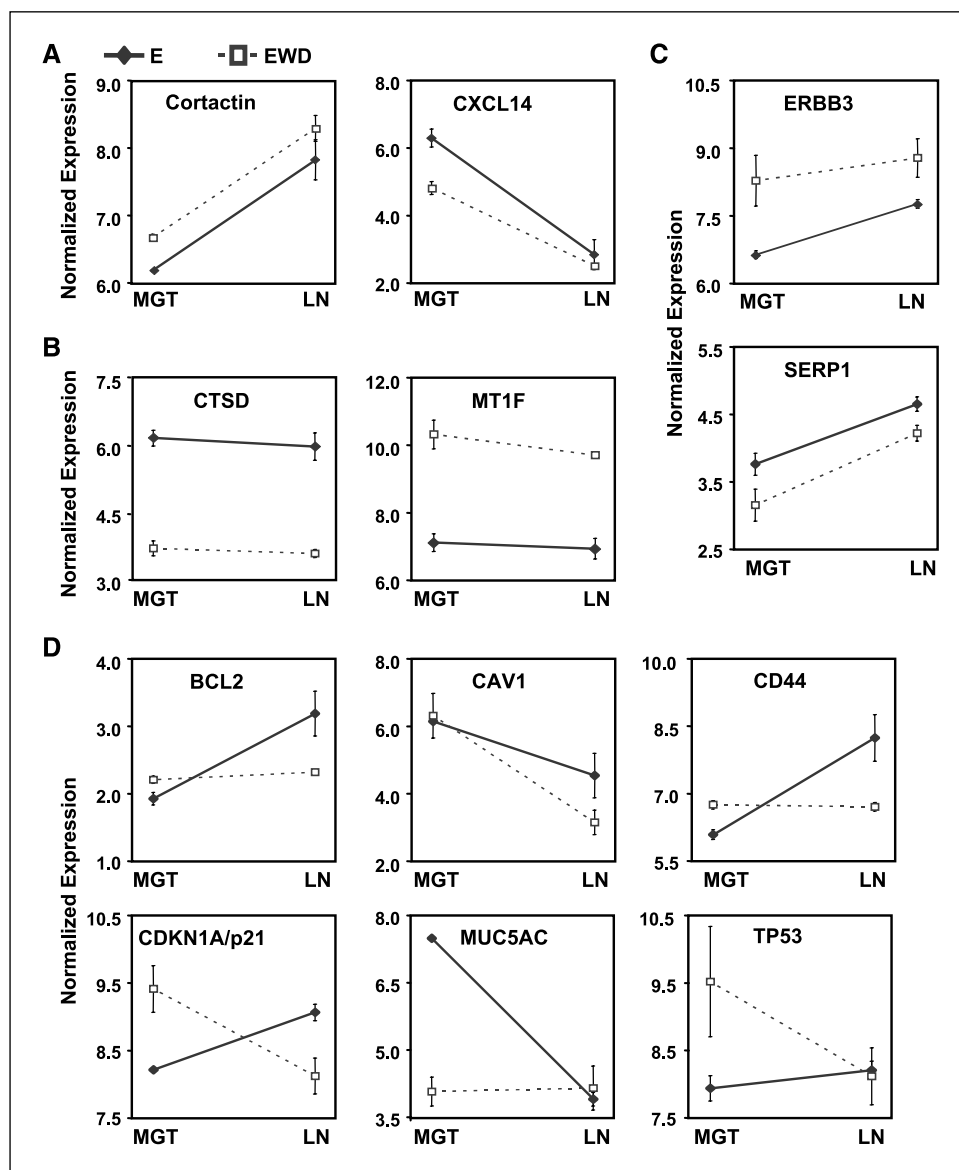
Figure 4. Genes that are tissue and hormone regulated with or without interaction effects. RMA normalized mean RNA expression values with SE. *Solid lines,* data from estradiol-treated tissues; *dashed lines,* data from EWD tissues. *A,* tissue-regulated genes. *B,* hormone-regulated genes. *MT1F,* metallothionein 1F. *C,* genes that are tissue and hormone regulated. *D,* genes with interaction effects that are differentially regulated by estradiol in the two tissues include *CAV1, MUC5AC, TP53, BCL2, CDKN1A*, and *CD44*.

Of the 1,570 differentially expressed transcripts, more had increased average expression in LN metastases (70%) than in primary tumors (30%). In addition, on average, genes were more highly expressed in EWD tissues (64%) than in estradiol-treated ones (36%), suggesting that estradiol affects approximately two thirds of genes through suppression of RNA levels. Among the 1,570 transcripts, 386 had only significant ($P < 0.05$; Fig. 3C) tissue effects, 44 had only significant hormone effects, and 91 were affected by both the tissue microenvironment and the presence of hormones (Fig. 3C). However, the majority of genes, 1,049 of 1,570, exhibited a significant interaction effect. The expression values of these genes could not be simply described as due to either of the main effects but rather due to an interrelationship between them. Most of these genes may also have significant main effects as shown by intersection in the Venn diagram, but interaction effects take precedence over these main effects, and the main effects cannot be correctly interpreted without acknowledging the inter-action effects (21). For these genes, expression levels in the two tissues (MGT and LN) were influenced differently by the type of hormone treatment (estradiol and EWD). A subset (145 of 1,049) of these genes exhibited only interaction effects.

Main effects and interaction effects can be visualized by graphical representation with levels of one factor on the *X* axis and separate lines representing levels of the other factor, as in Fig. 4. Lines that are parallel to one another with steep slopes or separation indicate main effects, whereas nonparallel lines indicate interaction effects. Figure 4A shows two examples of genes with significant tissue effects. Cortactin transcripts had significantly higher expression levels in LN metastases, regardless of hormone, as did the majority (290 of 386) of the tissue-regulated genes (other examples include *MAPK* and *cyclin F*). *CXCL14* is one of the 96 of 386 tissue-regulated genes whose levels were higher in the primary tumors compared with LN metastases.

Figure 4B shows two examples of genes with a significant hor-mone effect. The expression of cathepsin-D (CTSD) transcripts was dependent on estradiol regardless of the microenvironment. Other genes with similar expression patterns were *insulin-like growth factor-I receptor* (*IGF-IR*), *cadherin-15*, and *defensin β-1*. Transcript

levels of *metallothionein 1F* were suppressed by estradiol regardless of the microenvironment. Other examples of estradiol-suppressed genes are *cathepsin F* and *BLNK*.

A subset of differentially expressed genes (91 of 1,570) had RNA expression levels that were both hormone and tissue regulated as shown in Fig. 4*C*. *ERBB3* was significantly suppressed by estradiol regardless of the microenvironment, but its expression was also increased in LN metastases compared with MGTs of both hormone treatments. *SERP1* was also significantly increased in LN metastases compared with MGTs regardless of the presence of estradiol and was also significantly up-regulated by estradiol in both tissues.

The majority of differentially expressed genes (1,049 of 1,570) had a significant interaction effect, exhibiting an interrelationship between tissue and hormonal factors. Figure 4*D* shows examples of a few such genes. Transcripts for *BCL2, CAV1, CD44, CDKN1A, MUC5AC*, and *tumor promoter 53* (*TP53*) all exhibit interaction effects and are affected differently by estradiol in tumors and LN metastases. *MUC5AC* and *TP53* are examples of genes exhibiting main effects (hormone and tissue) but with the interaction term predominating. Main effects of *CDKN1A* (*p21*) cancel each other out, leaving the dominant role of interaction effects evident.

Immunohistochemistry. Several of the genes that were identified by the expression profiling analysis were investigated further at the protein level by immunohistochemistry (Fig. 5). The estradiol-regulated gene *CTSD* was expressed in 80% to 90% of estradiol-treated MCF-7 primary tumor cells, and EWD reduced this number to 50% to 60%. In the LN metastases in the presence of estradiol, 50% to 60% of cancer cells expressed CTSD; this fell to 10% to 15% on EWD (Fig. 5, *top*). CAV1 protein was unaffected by EWD but was expressed only in MGTs and not in LN metastases (Fig. 5, *middle*). In estradiol-treated tumors, CD44 was heterogeneously expressed; on EWD, nonsignificant increases in the percentage of CD44⁺ cells were recorded. Interestingly, the opposite pattern was observed in LN metastases. The extensive overexpression of CD44 in estradiol-treated cancer cells metastatic to LNs (15) is dramatically reduced by EWD (Fig. 5, *bottom*).

Estrogen-regulated genes. Two linear contrasts were done among the 1,570 differentially expressed transcripts comparing estradiol-treated with EWD tumors and estradiol-treated with EWD LN metastases (Fig. 6*A* and *B*). This identified transcripts that were estradiol regulated in MGTs compared with LN metastases. There were 273 significantly hormonally up-regulated or down-regulated genes (fold change >1.3; *P* < 0.025; Fig. 6*A*). Of these, 256 were estradiol dependent in tumors, 41 were estradiol dependent in LN metastases, and 24 maintained estradiol sensitivity in both MGTs and LN metastases (Fig. 6*A*). These data confirm the conclusions drawn from Figs. 2 and 3*A* that tumor cells in the LN microenvironment are relatively estradiol resistant.

To identify genes with any absolute difference in expression due to estradiol in MGTs and LN metastases, the fold change criterion was removed from the two linear contrasts. This increased the total list of significantly (*P* < 0.025) hormone-regulated genes from 273 to 1,176 (Fig. 6*B*). These additional 903 genes were up-regulated or down-regulated with fold changes >1.0 and <1.3, and in total, there were 707 estradiol-regulated genes in MGTs, 177 estradiol-regulated in LN metastases, and 292 estradiol-regulated in both sites. Seventy-five of these transcripts were regulated by estradiol in opposite directions in MGTs and LN metastases (Fig. 6*C*). *BCL2, CD44*, and *CDKN1A* are examples of such genes (Fig. 4*D*). *CDKN1A*, also known as *p21/WAF*, encodes a potent cyclin-
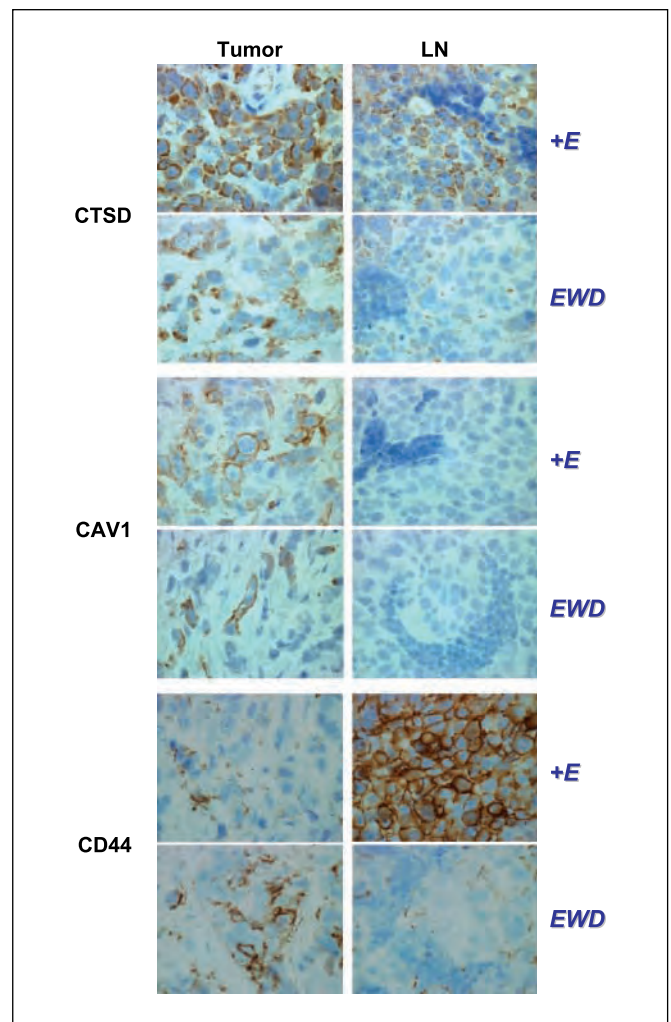
Figure 5. Immunohistochemical analyses of proteins that are hormone and tissue regulated. Estradiol-treated and EWD tumors and matched LN metastases from the same mouse were paraffin embedded, sectioned, and probed with CTSD, CAV1, or CD44 primary antibodies coupled with goat anti-rabbit or goat anti-mouse HRP-conjugated secondary antibodies. *Top*, estradiol-regulated CTSD; *middle*, CAV1 protein regulation by the tissue microenvironment; *bottom*, differential estradiol regulation of CD44 expression in tumors and LN metastases.

dependent kinase inhibitor and regulator of cell cycle progression at G_1. Its expression is tightly controlled by *TP53*, one of our set of microenvironment-regulated genes (Fig. 4*D*). CD44 (Fig. 5) is a putative breast cancer stem cell marker (22) and may target tumor cells to LNs (15).

Network analysis. Ingenuity data analysis was conducted to determine if the genes that had interaction effects and were differentially regulated by estradiol in MGTs and LN metastases are also involved in important functional networks. Twenty-seven unique gene networks that contained at least one differentially regulated gene were identified. Supplementary Fig. S1 shows a network of 33 genes, 100% of which are differentially estradiol regulated in MGTs and LN metastases. This network has TP53 at its center and functions in cellular responses to "therapeutics, cell death, and connective tissue disorders." Most of these genes (25 of 33) were estradiol regulated in MGTs but lost estradiol sensitivity in LN metastases (orange outline). Two genes were estradiol regulated in LN metastases but not in tumors (red outline), and the

remaining seven genes were regulated in the opposite direction by estradiol in MGTs and LN metastases (blue outline).

Discussion

Gene expression changes in MGTs and LN metastases. Two major theories have been advanced to explain successful cancer metastasis. (*a*) The "rare tumor cell hypothesis" states that only certain cells within tumors are capable of migrating and/or growing at distant sites. These rare cells may be stem cells, such as those that express CD44 (22). On the other hand, they may represent rare cells within a population of genetically diverse and unstable cells that originated with or acquired the appropriate genetic information needed to seed at specific metastatic sites (23). (*b*) An alternative hypothesis posits that metastatic capacity is an inherent rather than an acquired feature of breast cancers (24, 25) and is based on data suggesting that metastatic capacity is encoded early in the majority of cells within a tumor. In support of this idea are studies showing that tumors and their LN metastases retain similar genetic signatures, including aggressiveness and proliferation markers (24, 26, 27). One study, for example, found only 27 changed genes between lung tumors and their LN metastases (28). Weigelt et al. (27) identified a 70-gene cluster in primary breast tumors that predicts likelihood of subsequent metastases because the unique expression profiles of these genes were maintained in LNs and more distant metastases. Another study found no "shared genes" between primary tumors that were predictive of LN metastases but, anywhere between 3 and 149 genes, were "antiexpressed" or expressed in opposite directions in tumors versus LN metastases (29).

Our data provide evidence in support of both theories. In these studies, we analyze the changes in gene expression induced by estradiol as revealed by estradiol removal. Fewer than 5% of all genes analyzed were differentially expressed in cancer cells within the mammary gland compared with the LN. Although this might be considered a subtle difference, it nevertheless represents differential regulation of >1,000 genes in these two microenvironments. These genetic differences could be sufficient to define a "metastatic stem cell" (30), expressing the adaptive proteins required for successful colonization and growth of a subpopulation in a metastatic microenvironment, as envisioned by the rare tumor cell hypothesis. Elevated expression levels of the hyaluronan receptor CD44, a putative cancer stem cell marker, in estradiol-treated LN metastases suggest such selectivity in our models. On the other hand, our observations that cancer cell emboli move in bulk through LVs to LNs (15), coupled with our findings here and those of others (24, 27, 29) of modest genetic changes between primary tumors and LN metastases, could be interpreted as supporting the view that the majority of primary tumor cells arise either with or without the predisposition for LN spread. If true, the gene expression changes we observe could be attributed to the plasticity that all tumor cells exhibit when growing in two distinct microenvironments. Evidence supporting these microenvironmental effects on ER expression and function was found when a down-regulation "resistant" ER⁺ LN metastasis regained ER down-regulation capacity when grown in the mammary gland of a recipient mouse (Fig. 3*A*).

ER function in metastases. Beatson (31) reported >100 years ago that an essential feature of breast cancer is continuous and excessive growth of the epithelium, which invades the surrounding tissues, spreads along the LVs, passes from one set of LNs to another, and eventually forms deposits in distant organs, steps that occur more rapidly and prove to be more quickly fatal in younger patients. Knowing that the ovaries produced factors required for lactation, and believing "that all pathological changes are merely modified physiological ones," Beatson was the first to find that removal of the ovaries and the estradiol they elaborate reduced breast tumor size and extended the survival of young women with advanced breast cancer.

Seventy percent to 80% of primary breast cancers are ER⁺, and ∼80% of LN metastases retain the receptors (11–13, 32). If such tumors are treated with antiestrogens or EWD therapies, 20% to 50% acquire resistance (33), often recurring as LN metastases. Premenopausal women with LN metastases are less responsive to tamoxifen treatment than LN-negative patients (34), and nodal involvement is a significant predictor of local relapse (35) with a 5.6-fold higher relative risk of local recurrence than women with clear LNs. Preoperative chemotherapy causes significantly less damage to LN metastases in comparison with primary tumors (36). Based on these data, we hypothesized that ER effects on gene expression would be altered by the LN microenvironment. To the best of our knowledge, no previous studies have defined estradiol-regulated genes in tumors compared with their matched LN metastases. Identifying these genes is an important step toward elucidating mechanisms that contribute to breast cancer progression and estradiol resistance in advanced disease.

In the face of continuous estradiol treatment in two separate ER⁺ breast cancer cell lines, higher levels of ER were observed in LN metastases than in matched MGTs (Figs. 2 and 3*A*). The partial failure of ligand-dependent ER down-regulation in LN metastases suggests that the receptors are relatively estradiol insensitive in the LN microenvironment. Reduced PR expression in estradiol-treated LN metastases supports this conclusion, as does global gene expression profiling, which showed that estradiol had less influence on gene expression in LN metastases than in matched primary MGTs (Figs. 3 and 6). We have now identified numerous genes that are estradiol regulated in primary tumors but not in LN metastases. Examples include *MUC5A* and *TP53*, which were estradiol sensitive in MGTs but lost this regulation in the LNs. Additionally, 75 genes were regulated in the opposite direction by estradiol in MGTs compared with their LN metastases (Fig. 6*C*), 21 of which, including *BCL2* and *CDKN1A* (Fig. 4), were previously reported to be estradiol regulated (7, 37, 38). *CD44* (Figs. 4 and 5) was also regulated in opposite directions at the two sites. It is one of two cell surface markers that differentiate tumorigenic from nontumorigenic breast cancer cells (22). This putative stem cell and aggressiveness marker (39, 40) is an example of how EWD differentially alters the expression of a potential therapeutic target in primary tumors compared with LN metastases.

Mechanisms of estradiol resistance in LNs. Possible explanations for the differential estradiol sensitivity of MGTs versus LN metastases include increased availability of growth factors in LNs that directly interfere with ER transcription (41), diminished ubiquitination and loss of proteasome-mediated protein down-regulation in LNs (42, 43), loss of CAV1 and subsequent membrane signaling (44), and reduced estradiol availability to LNs. With regard to growth factors, IGFs and epidermal growth factors (EGF) activate the phosphatidylinositol 3-kinase-AKT-mammalian target of rapamycin pathways, which alter Jun and Fos activities at the PR promoter and decrease its ER-mediated transcription (45). LN stromal cells produce both IGF and EGF (41), which may explain the reduced PR induction as well as the reduced estradiol
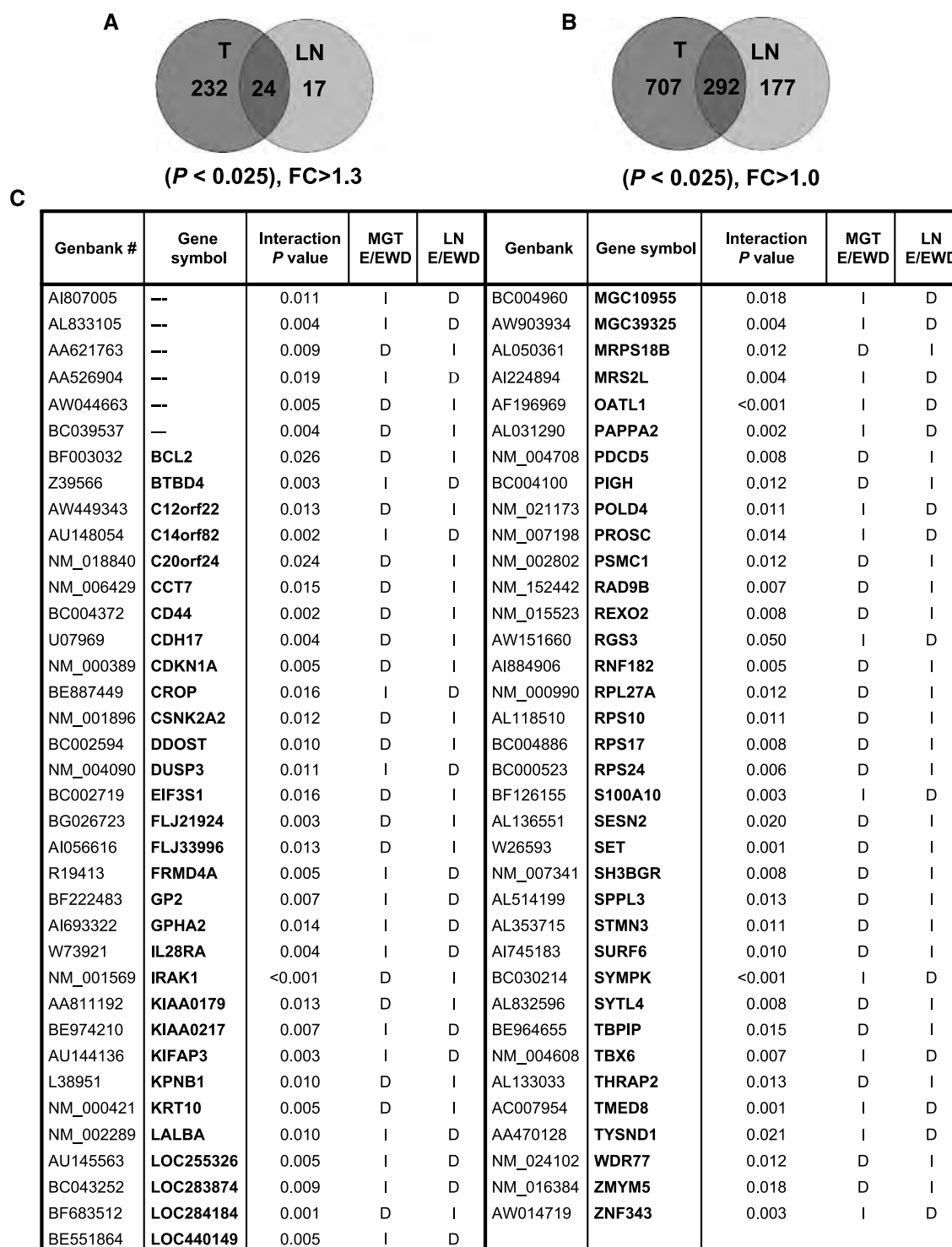
Figure 6. Pairwise comparisons to identify estradiol-regulated transcripts in tumors (*T*), LN metastases, or both. *A,* transcripts regulated in a significant manner ($P < 0.025$) by estradiol >1.3-fold. *B,* transcripts regulated in a significant manner ($P < 0.025$) by estradiol regardless of fold levels. *C,* list of 75 transcripts that are regulated in a significant manner in opposite directions by estradiol in MGTs compared with LN metastases. *I,* increases; *D,* decreases with estrogen.

The Venn diagrams and table referenced in Figure 6:

A: T 232 | 24 | LN 17, ($P < 0.025$), FC>1.3

B: T 707 | 292 | LN 177, ($P < 0.025$), FC>1.0

C:

Genbank #	Gene symbol	Interaction P value	MGT E/EWD	LN E/EWD	Genbank	Gene symbol	Interaction P value	MGT E/EWD	LN E/EWD
AI807005	—	0.011	I	D	BC004960	MGC10955	0.018	I	D
AL833105	—	0.004	I	D	AW903934	MGC39325	0.004	I	D
AA621763	—	0.009	D	I	AL050361	MRPS18B	0.012	D	I
AA526904	—	0.019	I	D	AI224894	MRS2L	0.004	I	D
AW044663	—	0.005	D	I	AF196969	OATL1	<0.001	I	D
BC039537	—	0.004	D	I	AL031290	PAPPA2	0.002	I	D
BF003032	BCL2	0.026	D	I	NM_004708	PDCD5	0.008	D	I
Z39566	BTBD4	0.003	I	D	BC004100	PIGH	0.012	D	I
AW449343	C12orf22	0.013	D	I	NM_021173	POLD4	0.011	I	D
AU148054	C14orf82	0.002	I	D	NM_007198	PROSC	0.014	I	D
NM_018840	C20orf24	0.024	D	I	NM_002802	PSMC1	0.012	D	I
NM_006429	CCT7	0.015	D	I	NM_152442	RAD9B	0.007	D	I
BC004372	CD44	0.002	D	I	NM_015523	REXO2	0.008	D	I
U07969	CDH17	0.004	D	I	AW151660	RGS3	0.050	I	D
NM_000389	CDKN1A	0.005	D	I	AI884906	RNF182	0.005	D	I
BE887449	CROP	0.016	I	D	NM_000990	RPL27A	0.012	D	I
NM_001896	CSNK2A2	0.012	D	I	AL118510	RPS10	0.011	D	I
BC002594	DDOST	0.010	D	I	BC004886	RPS17	0.008	D	I
NM_004090	DUSP3	0.011	I	D	BC000523	RPS24	0.006	D	I
BC002719	EIF3S1	0.016	D	I	BF126155	S100A10	0.003	I	D
BG026723	FLJ21924	0.003	D	I	AL136551	SESN2	0.020	D	I
AI056616	FLJ33996	0.013	D	I	W26593	SET	0.001	D	I
R19413	FRMD4A	0.005	I	D	NM_007341	SH3BGR	0.008	D	I
BF222483	GP2	0.007	I	D	AL514199	SPPL3	0.013	D	I
AI693322	GPHA2	0.014	I	D	AL353715	STMN3	0.011	D	I
W73921	IL28RA	0.004	I	D	AI745183	SURF6	0.010	D	I
NM_001569	IRAK1	<0.001	D	I	BC030214	SYMPK	<0.001	I	D
AA811192	KIAA0179	0.013	D	I	AL832596	SYTL4	0.008	D	I
BE974210	KIAA0217	0.007	I	D	BE964655	TBPIP	0.015	D	I
AU144136	KIFAP3	0.003	I	D	NM_004608	TBX6	0.007	I	D
L38951	KPNB1	0.010	D	I	AL133033	THRAP2	0.013	D	I
NM_000421	KRT10	0.005	D	I	AC007954	TMED8	0.001	I	D
NM_002289	LALBA	0.010	I	D	AA470128	TYSND1	0.021	I	D
AU145563	LOC255326	0.005	I	D	NM_024102	WDR77	0.012	D	I
BC043252	LOC283874	0.009	I	D	NM_016384	ZMYM5	0.018	D	I
BF683512	LOC284184	0.001	D	I	AW014719	ZNF343	0.003	I	D
BE551864	LOC440149	0.005	I	D					

regulation of other target genes at this site. Increased cortactin levels (Fig. 4) inhibit ubiquitin-mediated degradation of EGF receptors following their internalization, resulting in sustained ligand-induced EGF signaling (42, 43). It is possible that similar ubiquitin-dependent mechanisms explain the ER down-regulation defects we observe in LNs (Fig. 2; ref. 15). Supporting this hypothesis, nine transcripts known to be involved in the ubiquitination process were differentially expressed in MGTs and LN metastases.

28

This includes two known enzymes that function in the ubiquitination process, UBE2D3 and USP7, which were increased in LN metastases and also lost estradiol sensitivity in LN metastases (Supplementary Fig. S1). CAV1, a scaffold protein that transduces ER signaling at the plasma membrane (44), was decreased in LNs, possibly explaining loss of ER responsiveness. Finally, although it is possible that the diminished estradiol sensitivity of LN metastases is due to an overall decrease of estradiol levels within LNs, this is highly unlikely given the number of estradiol-regulated genes whose levels are maintained or increased in LN metastases (Fig. 4).

Networks. We speculated that genes differentially regulated in MGTs versus LN metastases may contribute to tumor aggressiveness, recurrence, and/or growth in LNs. We therefore analyzed the functional networks characterizing these genes. Of interest was a 33-gene network composed entirely of transcripts regulated differently by estradiol in MGTs and LNs (Supplementary Fig. S1), which included CDNK1A, TP53, and BCL2-linked signaling pathways. In this network, the majority of the genes were significantly regulated by estradiol in tumors while losing estradiol sensitivity in LN metastases or suppressed by estradiol in tumors but increased by estradiol in LN metastases. These findings are interesting given the fact that 70% of the 1,570 global genes differentially expressed in the two sites were increased in LN metastases compared with MGTs, whereas 64% of the differentially estradiol-regulated genes were suppressed by estradiol. This corroborates previous data with MCF-7 cells showing that 70% of genes are down-regulated by estradiol treatment (38) and is consistent with an overall lifting of the suppressive effects of estradiol in MCF-7 tumor cells growing in LNs. It is possible that these results do not completely mimic effects in a patient with an intact immune system. The LNs of nude mice lack or have reduced numbers of T cells (46). However, they have B cells, natural killer cells, reticular cells, and macrophages as well as a nodal stromal network and architecture. Because different substrata are known to alter growth and function of ER$^+$ human breast cancer cells *in vitro* (6), it is likely that the LN microenvironment, including its unique architecture, cytokines, and growth factors, modifies ER function. Given the experimental nature of our models, these findings stress the need for further studies to show whether estradiol insensitivity occurs in clinical ER$^+$ LN metastases and whether other metastatic microenvironments differentially modulate estradiol sensitivity and to define estradiol-regulated genes uniquely influenced by the microenvironment of tumor cells. This approach may identify key genes that can be targeted therapeutically at specific metastatic sites.

In summary, we describe a xenograft model of EWD after LN metastasis and show that estradiol regulation of genes is different in ER$^+$ primary MGTs compared with their matched ER$^+$ LN metastases. Through global gene expression profiling and immunohistochemical analyses, we identify genes that maintain, lose, or are regulated in the opposite direction by estradiol in tumors and LN metastases. These results suggest that current ER-targeted therapies may differentially affect tumor cells depending on the microenvironment in which the cells reside. If so, our studies provide possible new therapeutic targets, which, in combination with standard hormonal therapies, might improve responses of advanced breast cancers.

References

1. Novaro V, Radisky DC, Ramos Castro NE, Weisz A, Bissell MJ. Malignant mammary cells acquire independence from extracellular context for regulation of estrogen receptor α. Clin Cancer Res 2004;10:402–9S.

2. Mueller SO, Clark JA, Myers PH, Korach KS. Mammary gland development in adult mice requires epithelial and stromal estrogen receptor α. Endocrinology 2002;143:2357–65.

3. Hansen RK, Bissell MJ. Tissue architecture and breast cancer: the role of extracellular matrix and steroid hormones. Endocr Relat Cancer 2000;7:95–113.

4. Ronnov-Jessen L, Peterson OW, Bissell MJ. Cellular changes involved in conversion of normal to malignant breast importance of the stromal reaction. Physiological Reviews 1996;76:69–125.

5. Davidson B, Konstantinovsky S, Nielsen S, et al. Altered expression of metastasis-associated and regulatory molecules in effusions from breast cancer patients: a novel model for tumor progression. Clin Cancer Res 2004;10:7335–46.

6. Haslam SZ, Woodward TL. Host microenvironment in breast cancer development: epithelial-cell-stromal-cell interactions and steroid hormone action in normal and cancerous mammary gland. Breast Cancer Res 2003;5:208–15.

7. Harvell DM, Richer JK, Allred DC, Sartorius CA, Horwitz KB. Estradiol regulates different genes in human breast tumor xenografts compared with the identical cells in culture. Endocrinology 2006;147:700–13.

8. Vinh-Hung V, Verschraegen C, Promish DI, et al. Ratios of involved nodes in early breast cancer. Breast Cancer Res 2004;6:R680–8.

9. Veronesi U, Paganelli G, Viale G, et al. Sentinel lymph node biopsy and axillary dissection in breast cancer: results in a large series. J Natl Cancer Inst 1999;91:368–73.

10. Jatoi I, Hilsenbeck SG, Clark GM, Osborne CK. Significance of axillary lymph node metastasis in primary breast cancer. J Clin Oncol 1999;17:2334–40.

11. Zheng WQ, Lu J, Zheng JM, Hu FX, Ni CR. Variation of ER status between primary and metastatic breast cancer and relationship to p53 expression*. Steroids 2001;66:905–10.

12. Butler JA, Trezona T, Vargas H, State D. Value of measuring hormone receptor levels of regional metastatic carcinoma of the breast. Arch Surg 1989;124:1131–4; discussion 1134–5.

13. Hoehn JL, Plotka ED, Dickson KB. Comparison of estrogen receptor levels in primary and regional metastatic carcinoma of the breast. Ann Surg 1979;190:69–71.

14. Gartner LP, Hiatt JL. Color atlas of histology. 4th Ed. Philadelphia: Lippincott Williams & Wilkins; 2006; p. 167–86.

15. Harrell JC, Dye WW, Allred DC, et al. Estrogen receptor positive breast cancer metastasis: altered hormonal sensitivity and tumor aggressiveness in lymphatic vessels and lymph nodes. Cancer Res 2006;66:9308–15.

16. Sartorius CA, Groshong SD, Miller LA, et al. New T47D breast cancer cell lines for the independent study of progesterone B- and A-receptors: only antiprogestin-occupied B-receptors are switched to transcriptional agonists by cAMP. Cancer Res 1994;54:3868–77.

17. Sartorius CA, Shen T, Horwitz KB. Progesterone receptors A and B differentially affect the growth of estrogen-dependent human breast tumor xenografts. Breast Cancer Res Treat 2003;79:287–99.

18. McClintick JN, Edenberg HJ. Effects of filtering by present call on analysis of microarray experiments. BMC Bioinformatics 2006;7:49.

19. Horwitz KB, Koseki Y, McGuire WL. Estrogen control of progesterone receptor in human breast cancer: role of estradiol and antiestrogen. Endocrinology 1978;103:1742–51.

20. Lonard DM, Nawaz Z, Smith CL, O'Malley BW. The 26S proteasome is required for estrogen receptor-α and coactivator turnover and for efficient estrogen receptor-α transactivation. Mol Cell 2000;5:939–48.

21. Li H, Wood CL, Getchell TV, Getchell ML, Stromberg AJ. Analysis of oligonucleotide array experiments with repeated measures using mixed models. BMC Bioinformatics 2004;5:209.

22. Al-Hajj M, Wicha MS, Benito-Hernandez A, Morrison SJ, Clarke MF. Prospective identification of tumorigenic breast cancer cells. Proc Natl Acad Sci U S A 2003;100:3983–8.

23. Fidler IJ, Kripke ML. Metastasis results from pre-existing variant cells within a malignant tumor. Science 1977;197:893–5.

24. Perou CM, Sorlie T, Eisen MB, et al. Molecular portraits of human breast tumours. Nature 2000;406:747–52.

25. Bernards R, Weinberg RA. A progression puzzle. Nature 2002;418:823.

26. Lacroix M, Toillon RA, Leclercq G. Stable 'portrait' of breast tumors during progression: data from biology, pathology and genetics. Endocr Relat Cancer 2004;11:497–522.

27. Weigelt B, Hu Z, He X, et al. Molecular portraits and 70-gene prognosis signature are preserved throughout the metastatic process of breast cancer. Cancer Res 2005;65:9155–8.

28. Hoang CD, Guillaume TJ, Engel SC, Tawfic SH, Kratzke RA, Maddaus MA. Analysis of paired primary lung and lymph node tumor cells: a model of metastatic potential by multiple genetic programs. Cancer Detect Prev 2005;29:509–17.

29. Weigelt B, Wessels LF, Bosma AJ, et al. No common denominator for breast cancer lymph node metastasis. Br J Cancer 2005;93:924–32.

30. Balic M, Lin H, Young L, et al. Most early disseminated cancer cells detected in bone marrow of breast cancer patients have a putative breast cancer stem cell phenotype. Clin Cancer Res 2006;12:5615–21.

31. Beatson GT. On the treatment of inoperable cases of carcinoma of the mamma: suggestions for a new method of treatment, with illustrative cases. Lancet 1896;2:104–7.

32. Koda M, Sulkowski S, Kanczuga-Koda L, Surmacz E, Sulkowska M. Expression of ERα, ERβ and Ki-67 in primary tumors and lymph node metastases in breast cancer. Oncol Rep 2004;11:753–9.

33. Arpino G, Weiss H, Lee AV, et al. Estrogen receptor-positive, progesterone receptor-negative breast cancer: association with growth factor receptor expression and tamoxifen resistance. J Natl Cancer Inst 2005;97:1254–61.

34. Ahn SH, Son BH, Kim SW, et al. Poor outcome of hormone receptor-positive breast cancer at very young age is due to tamoxifen resistance: nationwide survival data in Korea—a report from the Korean Breast Cancer Society. J Clin Oncol 2007;25:2360–8.

35. van Dongen JA, Bartelink H, Fentiman IS, et al. Factors influencing local relapse and survival and results of salvage treatment after breast-conserving therapy in operable breast cancer: EORTC trial 10801, breast conservation compared with mastectomy in TNM stage I and II breast cancer. Eur J Cancer 1992;28A:801–5.

36. Koda M, Lenczewski A, Sulkowska M, et al. The effect of chemotherapy on status of estrogen receptors in primary tumors and lymph node metastases of human ductal breast cancer. Oncol Rep 2007;17:385–91.

37. Creighton CJ, Cordero KE, Larios JM, et al. Genes regulated by estrogen in breast tumor cells *in vitro* are similarly regulated *in vivo* in tumor xenografts and human breast tumors. Genome Biol 2006;7:R28.

38. Frasor J, Danes JM, Komm B, Chang KC, Lyttle CR, Katzenellenbogen BS. Profiling of estrogen up- and down-regulated gene expression in human breast cancer cells: insights into gene networks and pathways underlying estrogenic control of proliferation and cell phenotype. Endocrinology 2003;144:4562–74.

39. Li C, Heidt DG, Dalerba P, et al. Identification of pancreatic cancer stem cells. Cancer Res 2007;67:1030–7.

40. Liu S, Dontu G, Mantle ID, et al. Hedgehog signaling and Bmi-1 regulate self-renewal of normal and malignant human mammary stem cells. Cancer Res 2006;66:6063–71.

41. LeBedis C, Chen K, Fallavollita L, Boutros T, Brodt P. Peripheral lymph node stromal cells can promote growth and tumorigenicity of breast carcinoma cells through the release of IGF-I and EGF. Int J Cancer 2002;100:2–8.

42. Timpson P, Lynch DK, Schramek D, Walker F, Daly RJ. Cortactin overexpression inhibits ligand-induced down-regulation of the epidermal growth factor receptor. Cancer Res 2005;65:3273–80.

43. van Rossum AG, Gibcus J, van der Wal J, Schuuring E. Cortactin overexpression results in sustained epidermal growth factor receptor signaling by preventing ligand-induced receptor degradation in human carcinoma cells. Breast Cancer Res 2005;7:235–7.

44. Levin ER, Pietras RJ. Estrogen receptors outside the nucleus in breast cancer. Breast Cancer Res Treat. Epub 2007 Jun 26.

45. Petz LN, Ziegler YS, Schultz JR, Nardulli AM. Fos and Jun inhibit estrogen-induced transcription of the human progesterone receptor gene through an activator protein-1 site. Mol Endocrinol 2004;18:521–32.

46. Giovanella BC, Fogh J. The nude mouse in cancer research. Adv Cancer Res 1985;44:69–120.

RESEARCH PAPER

Contaminating cells alter gene signatures in whole organ versus laser capture microdissected tumors: a comparison of experimental breast cancers and their lymph node metastases

**Joshua Chuck Harrell · Wendy W. Dye ·
Djuana M. E. Harvell · Carol A. Sartorius ·
Kathryn B. Horwitz**

Abstract Genome-wide expression profiling has expedited our molecular understanding of the different subtypes of breast cancers, as well as defined the differences among genes expressed in primary tumors and their metastases. Laser-capture microdissection (LCM) coupled to gene expression analysis allows us to understand how specific cell types contribute to the total cancer gene expression signature. Expression profiling was used to define genes that contribute to breast cancer spread into and/or growth within draining lymph nodes (LN). Whole tumor xenografts and their matched whole LN metastases were compared to LCM captured cancer cells from the same tumors and matched LN metastases. One-thousand nine-hundred thirty genes were identified by the whole organ method alone, and 1,281 genes by the LCM method alone. However, less than 1% (30 genes) of genes that changed between tumors and LN metastases were common to both methods. Several of these genes have previously been implicated in cancer aggressiveness. Our data show that whole-organ and LCM based gene expression profiling yield distinctly different lists of metastasis-promoting genes. Contamination of the tumor

cells, and cross reactivity of mouse RNA to human-specific chips may explain these differences, and suggests that LCM-derived data may be more accurate.

Abbreviations

CK18	Cytokeratin 18
ER	Estrogen receptor
H & E	Hematoxylin and eosin
LCM	Laser-capture microdissection
LN	Lymph node

J. C. Harrell (✉) · W. W. Dye · D. M. E. Harvell ·
C. A. Sartorius · K. B. Horwitz
Division of Endocrinology, Department of Medicine, University
of Colorado Health Sciences Center, MS 8106, RC-1 South,
12801 E. 17th Ave, Room 7402G, PO Box 6511, Aurora,
CO 80045, USA
e-mail: Joshua.Harrell@uchsc.edu

K. B. Horwitz
Department of Pathology, University of Colorado Health
Sciences Center, Aurora, CO, USA

J. C. Harrell · K. B. Horwitz
Program in Reproductive Sciences, University of Colorado
Health Sciences Center, Aurora, CO, USA

Introduction

Breast cancer metastasis kills over 400,000 worldwide each year [1]. At diagnosis, 30–50% of primary breast cancers have disseminated to other locations including the draining lymph nodes (LN). Assessments of tumor aggressiveness as predictors of overall survival were historically confined to histological evaluations by trained pathologists. More recently, molecular approaches have been shown to be superior to pathological staging to determine patient prognosis and treatment options [1–5].

Through global gene expression profiling, breast cancers have been shown to be derived from at least two functionally distinct cell types, basal cells and luminal epithelial cells; each responds differently to therapeutics [6]. From these genome-wide analyses new hypotheses have been proposed, which suggest that the ability of a breast cancer cell to metastasize is intrinsically encoded

and linked to the same genetic alterations that initiated the growth of the primary tumor [7, 8]. Alternatively, other data indicate that only certain 'rare cells' within a breast tumor harbor the potential for tumor growth and metastasis [9]. It is possible that both views of progression are correct and that tumors that generate metastatic cells differ only slightly in their transcriptome from the bulk of the cells that comprise the primary tumor.

A large number of studies have been conducted to identify the genes that are expressed differently in primary tumors compared to their metastases, and that may therefore contribute to increased aggressiveness. Interestingly, the published 'metastatic gene profiles' are not composed of the same gene lists [10]. Among other things, these differences among studies have been attributed to tissue sampling variations or to different statistical analyses [10].

We have been engaged in identifying genes that may be responsible for the spread and/or growth of estrogen receptor (ER) positive breast cancers to the LNs. To this end we determined if the two commonly used methods to isolate RNA—whole-organ isolation and laser-capture microdissection (LCM)—identify similar sets of genes in an experimental model. We find that using the same tumor lines and statistical analyses, gene expression profiles from whole-organs are completely different from the profiles using LCM isolated cells, with only minor overlap between them. Some of the overlapping genes have been previously shown to be involved in cancer aggressiveness. We conclude that the methods used to isolate RNA can markedly skew the results obtained.

Materials and methods

Fluorescent xenograft model of ER + LN metastasis

ER+ MCF-7 human breast cancer cells were originally purchased from the American Type Culture Collection (Manassas, VA). The generation of fluorescent MCF-7 cells has been previously described [11]. In brief, ZsGreen retroviral particles (Clontech, Mountain View, CA) were isolated from PT-67 packaging cells (Clontech), filtered, and overlaid onto MCF-7 cells. Cells were serially transduced and then subjected to G418 selection, followed by aseptic fluorescence associated cell sorting to isolate a homogeneously bright green subpopulation.

All animal procedures were performed under a protocol approved by the University of Colorado Institutional Animal Care and Use Committee. Ovariectomized athymic nu/nu mice were obtained from Harlan Sprague-Dawley (Indianapolis, IN) at 5–6 weeks of age. To establish tumors, mice were anesthetized with Avertin and injected into the opening of the lactiferous duct of the abdominal

mammary glands with 1 million ZsGreen-expressing MCF-7 cells in 100 microliters of 100% Matrigel (Becton Dickinson, Franklin Lakes, NJ). Mice were also implanted with silastic pellets containing 17β-estradiol (2 mg + 8 mg cellulose) as previously described [12]. Fluorescent whole-body imaging (Illumatool 9900, Lightools Research, Encinitas, CA) was done weekly to determine when axillary LN metastases arose. Mice were euthanized by CO_2 asphyxiation and fluorescent intravital optical imaging was done by coupling the Illumatool with an Olympus (Melville, NY) SZ-61 dissecting microscope and Olympus C-5050 digital camera. Fluorescent tumors in mammary glands and matched LN metastases were removed.

Whole-organ RNA isolation and expression profiling

Tumors in mammary glands and LNs containing metastases were extracted and frozen at –80°C. RNA was prepared with Trizol according to the manufacturer's specifications (Invitrogen, Carlsbad, CA). Samples were in vitro transcribed, biotinylated, hybridized to Affymetrix HG-U133+2 chips that interrogate 47,000 transcripts with 54,675 probesets (Santa Clara, CA), and scanned on an Agilent bioanalyzer 2100 (Santa Clara, CA).

Laser-capture microdissection, RNA isolation and expression profiling

Mammary gland tumors and LNs containing metastases were harvested, placed in a Tissue Tek cryomold (EMS, Hatfield, PA), covered with Neg50 frozen section medium (Richard-Allan Scientific, Kalamazoo, MI), and frozen in isopentane (Sigma, St. Louis, MO) cooled by liquid nitrogen. Eight micron sections were cut through the entire tumor or LN with a cryotome set at –20°C. Each section was collected on an uncharged slide (Fisher), and every 10th slide was stained for hematoxylin and eosin (H & E) or processed for cytokeratin 18 (CK18) immunofluorescence to confirm location of the cancer cells. Serial sections of slides containing cancer cells were processed through 75% ethanol, water, 75, 95, and 100% ethanol for 30 s each, and finally dehydrated with xylene for 1 min before being immediately subjected to laser-capture microdissection using an Arcturus Autopix (Sunnyvale, CA). Two-thousand cells for each sample were extracted within 30 min of fixation and frozen at –70°C until further processing. Suggested protocols from Arcturus were followed for RNA extraction and two rounds of amplification using the Picopure RNA isolation kit and RiboAmp HS kit (Arcturus), respectively. Samples were in vitro transcribed, biotinylated, hybridized to Affymetrix (Santa Clara, CA)

human X3P chips that interrogate 47,000 transcripts with 61,358 probesets, and scanned on an Agilent (Santa Clara, CA) bioanalyzer 2100.

Statistical analyses

The data from four whole-organ chips (two pairs of tumors and their matched LNs), and four LCM chips (two pairs of tumors and their matched LNs) were imported into Partek (Genomics Suite software St. Louis, MO) and RMA normalized. For comparative analyses between the whole-organ and LCM data, matching probesets from the two different chip types were identified. Of the 54,675 U133+2 probesets, 3,487 were dropped from the analysis because there was no X3P match, but 7,301 probesets were used multiple times. The result was that all but 62 of the 61,358 X3P probesets were matched to a U133+2 probeset. The expression values for each organ corresponding to either the U133+2 or X3P probeset were exported into Microsoft Excel (Redmond, WA). An array-comparison datasheet that matched the U133+2 probesets to the X3P probesets was obtained from Affymetrix. Using this program the RMA normalized expression values from Partek for the four U133+2 chips were matched to the corresponding X3P probesets of the four X3P chips. This resulted in normalized expression levels from all eight chips. The chip data were also imported into Genespring (Agilent) to obtain present/marginal/absent calls for each chip. Probesets with absent calls on all eight chips of the same type were excluded from analysis leaving 36,682 genes that were present on one of the eight chips for analysis. These genes were imported into Partek according to the X3P probeset identifiers. Separate paired t-tests were performed on the whole-organ and LCM matched primary tumor and LN pairs. P-values <0.05 were considered significant.

Gene networking analyses

To define relationships among genes that were differentially regulated in tumors versus LN metastases, pathway analyses were performed using Ingenuity software (Redwood City, CA). Probeset identification numbers from transcripts with increased or decreased expression in LN metastases were used for gene identification.

Results

Tissue acquisition

Estrogen-dependent MCF-7 tumor growth is required for LN metastasis [11]. For these studies MCF7 + ZsGreen cells were grown in the mammary gland of ovariectomized immunocompromised mice that had been supplemented with an estradiol releasing pellet. Identification of axillary LN metastases was achieved with fluorescent whole body imaging (Fig. 1a). At 12 weeks intact mammary gland tumors (Fig. 1b) and their matched LN metastases (Fig. 1c) were harvested and frozen as intact whole-organs or cut into 8-micron frozen sections. LNs and tumors were then probed with a breast cancer cell marker, cytokeratin 18, to map cancer cell locations (Fig. 1d). Adjacent sections were then used for LCM (Fig. 1e–g). The LN metastases that were used for the intact whole-organ analysis contained approximately equal amounts of cancer cells as assessed by ZsGreen fluorescence, CK18 immunohistochemistry, and H&E staining.

Gene expression profiling

To compare gene expression signatures in whole tumors and matched intact LN metastases, a paired t-test was performed. With this approach 1,930 genes were identified as being differentially expressed in tumors compared to LN metastases, with 1,213 decreased and 717 increased in the metastases compared to the tumors from which they originated (Fig. 2a). For the LCM samples, the same procedures were followed, which identified 368 decreased transcripts and 913 increased transcripts in the metastases compared to the tumors from which they originated (Fig. 2b). Clearly the pattern of upregulation and downregulation differs in the two types of analyses. Additionally, the volcano plots show much larger differences in 'fold-changes' between tumors and LN metastases that were laser-captured compared to the whole-organ samples.

Genes that change in whole-organ compared to LCM

When whole-organ and LCM paired t-test results were combined, 3,181 transcripts were found to have significantly increased or decreased expression levels in tumors versus LN metastases. Of the 3,181 however, only 68 (2%) were identified as changing by both analyses (Fig. 3a), and when the direction of change was calculated for these 68 transcripts; 38 were found to change in opposite directions by the two analyses (Fig. 3a). The remaining 30 transcripts (~1% of all genes) that changed in the same direction in both the whole-organ and LCM analyses are listed in Table 1.

Results from the paired t-tests were compared to identify all transcripts that were differentially regulated in either whole-organ or LCM analyses. Using both data sets, 1,570

Fig. 1 Isolation of tumors and LN metastases used for "whole-organ" or laser-capture microdissection followed by gene expression profiling. (**a**) Fluorescent whole body image of an immunocompromised mouse with bilateral MCF7 + ZsGreen tumors and an axillary LN metastasis, (**b**) ex vivo fluorescent image of a MCF7 + ZsGreen tumor, (**c**) LN metastasis, (**d**) cytokeratin 18 immunohistochemistry of an axillary LN metastasis, CK18 red, DAPI, blue, (**e**) hematoxylin and eosin stain of a LN identifying the metastatic MCF7 + ZsGreen cells (*), (**f**) combined images of a serial section of **d** with the cancer cells marked for LCM, (**g**) Post-LCM image of captured MCF7 cells from **e**
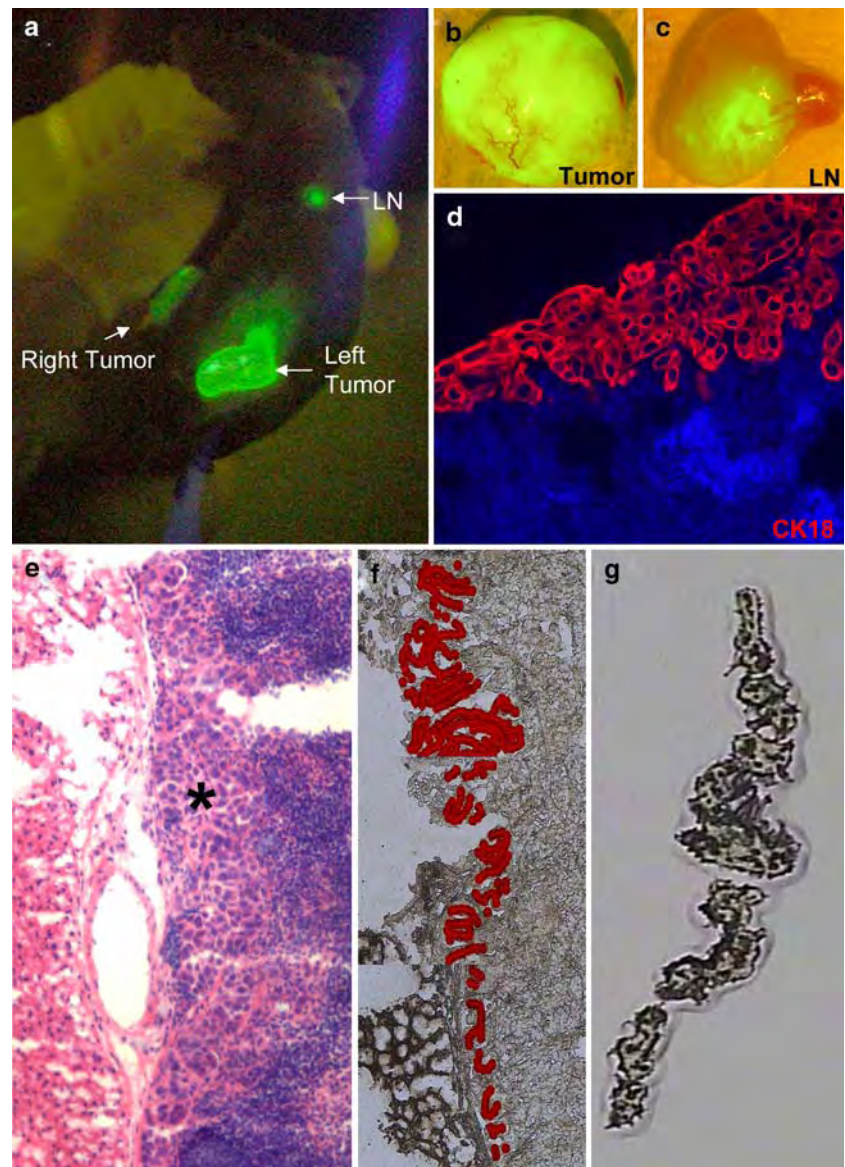
transcripts were found to be downregulated in LN metastases (Fig. 3b). Of these, 1,202 were unique to the whole-organ analysis, 357 were unique to LCM analysis, and 11 genes exhibited decreased expression with either method. A similar trend was observed among 1,611 genes that were upregulated in LN metastases, with 698 being whole-organ specific, 894 being LCM specific, and 19 common to the two analyses (Fig. 3c).

Ingenuity pathway analyses were performed to determine if the large differences between the two types of analyses could nevertheless be due to changes among similar functional networks. The whole-organ data identified pathways encoding GM-CSF signaling, insulin receptor signaling, amyloid processing, Jak/Stat signaling, and sonic hedgehog signaling that were the most different in the LN metastases. The LCM data identified completely different pathways that had changed the most in LN metastases including PI3K/AKT signaling, PTEN signaling, synthesis and degradation of ketone bodies, oxidative phosphorylation, and keratin sulfate biosynthesis. Clearly both the individual genes and the broader pathways that are altered in tumors versus LN metastases are different depending on the assays that are performed.
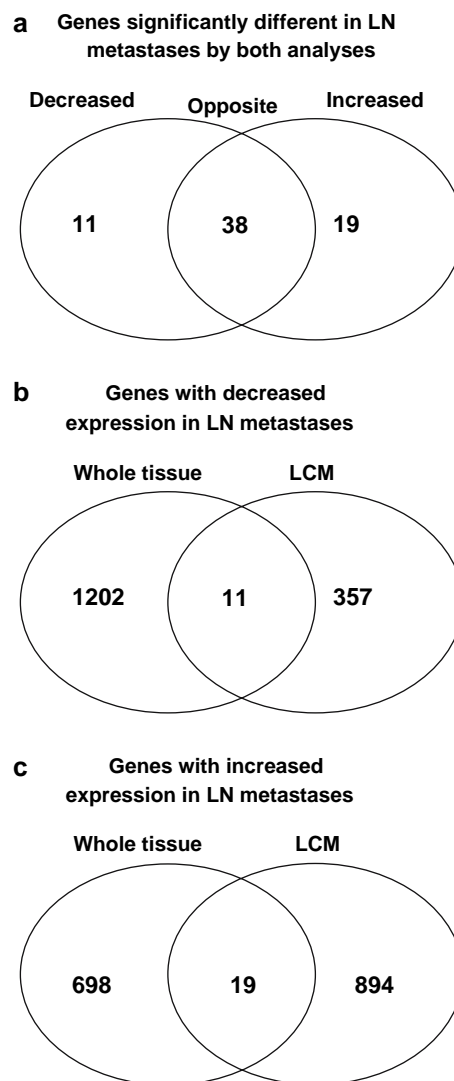
Discussion

Numerous studies from independent labs have shown that there are gene expression changes in cancer cells within primary tumors compared to cells that seed to different metastatic microenvironments [8, 13]. These studies suggest that the propensity for development of metastasis is

a **Change in LN metastases gene expression**
(whole-tissue)

b **Change in LN metastases gene expression**
(laser-captured)
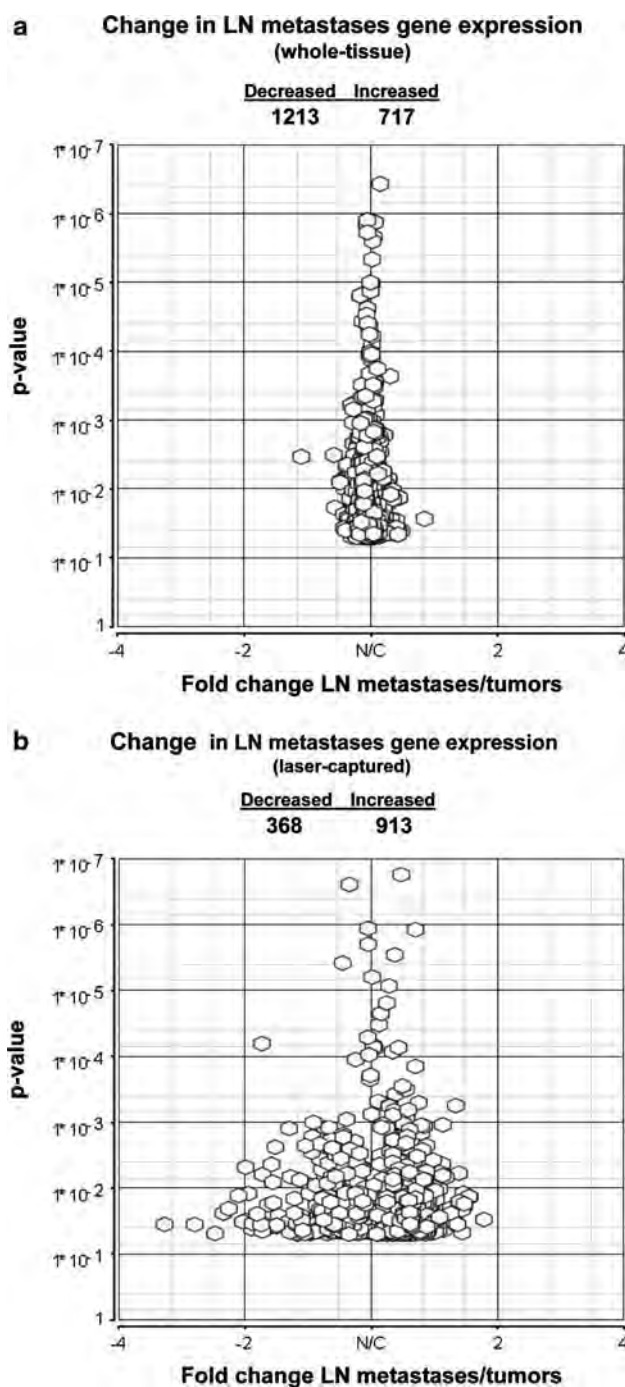
Fig. 2 Identification of the magnitude of gene expression changes in tumors and LN metastases. (**a**) Volcano plot showing the 1,930 genes that were significantly different between tumors and LN metastases in the whole-organ analysis, (**b**) volcano plot showing the 1,281 genes that were significantly different between tumors and LN metastases by the LCM analysis. For both plots the magnitude of fold change is shown on the *x*-axis and the significance is shown on the *y*-axis

due to genes that are altered during the initial tumorigenic process. The genetic changes in metastases have been attributed to differences required for successful colonization and growth within vastly different metastatic

a **Genes significantly different in LN metastases by both analyses**

b **Genes with decreased expression in LN metastases**

c **Genes with increased expression in LN metastases**

Fig. 3 Determining the overlap of the genes that changed in the whole-organ and LCM analyses. Significantly changing genes have a decrease or increase in the direction of the fold change without specifying a cut-off value. (**a**) Categorization of the 68 genes that were changed in both whole-organ and LCM analyses. Shown are genes that decreased or increased in LN metastases with both analyses or those whose expression changed in the opposite direction in each analysis, (**b**) genes with decreased expression in LN metastases, (**c**) genes with increased expression in LN metastases

microenvironments [14]. Whether the cells that are capable of metastasis are 'rare cells' or 'cancer stem-cells', or reflect any cell within the tumor, remains under debate [8, 9]. Regardless, determining the genes that are differentially expressed between cancer cells growing within the breast compared to those growing in other sites is crucial to understanding the mechanisms that allow cells to seed and grow at distant sites. Identifying these genes and rendering them therapeutic targets, is an essential first step towards inhibiting lethal metastases.

Table 1 Genes that increased or decreased in LN metastases by both analyses

X3P PSID	UniGene ID	Gene symbol	Whole-tissue FC(LN/MGT)	LCM FC(LN/MGT)
Genes with increased expression in LN metastases in both analyses				
219529_3p_at	Hs.64746	CLIC3	1.1114	1.0972
Hs2.429028.1.S1_3p_at	Hs.632184	CARHSP1	1.0548	1.0498
g11545730_3p_at	Hs.112569	GAN	1.0492	1.1879
g4557696_3p_a_at	Hs.99936	KRT10	1.0431	1.2789
208549_3p_x_at	Hs.591909	PTMA	1.0376	1.1448
g4507574_3p_a_at	Hs.279594	TNFRSF1A	1.0373	1.1685
g388890_3p_a_at	Hs.89643	TKT	1.0285	1.2193
g9295191_3p_s_at	Hs.584881	C3orf28	1.0242	1.3023
g12804874_3p_a_at	Hs.226390	RRM2	1.0222	1.3370
g4505038_3p_at	Hs.1116	LTBR	1.0181	1.1803
Hs.121017.0.S1_3p_at	Hs.121017	HIST1H2AE	1.0171	1.3161
g7959918_3p_a_at	Hs.381126	RPS14	1.0153	1.2751
Hs.27931.0.S1_3p_at	Hs.592295	GNPNAT1	1.0083	1.1926
g7705770_3p_at	Hs.19385	ABHD5	1.0062	1.3309
Hs.27239.0.S1_3p_at	Hs.27239	ZDHHC5	1.0057	1.1618
201217_3p_x_at	Hs.119598	RPL3	1.0050	1.1517
211073_3p_x_at	Hs.119598	RPL3	1.0043	1.1548
g13623708_3p_s_at	Hs.119598	RPL3	1.0042	1.1483
g4501976_3p_a_at	Hs.512815	AP3D1	1.0028	1.2395
Genes with decreased expression in LN metastases in both analyses				
Hs.74034.1.S1_3p_at	Hs.74034	CAV1	−1.14927	−1.21563
Hs.24812.0.S1_3p_at	Hs.472027	CDS2	−1.01957	−1.06974
Hs.172329.1.S1_3p_at	Hs.485628	ZNF451	−1.01761	−1.06306
Hs.161962.0.S1_3p_at	Hs.370510	IGSF4	−1.03359	−1.01245
Hs.145612.0.S2_3p_at	Hs.190622	DDX58	−1.05818	−1.26471
Hs.106440.0.A1_3p_at	–	–	−1.07679	−1.05797
g9951924_3p_at	Hs.210995	CA12	−1.08361	−1.05245
g7661679_3p_a_at	Hs.455336	NELF	−1.01845	−1.04308
g4929370_3p_x_at	Hs.465885	ILF3	−1.0444	−1.0716
g12052731_3p_x_at	Hs.351906	ZNF506	−1.04132	−1.0935
g12052731_3p_at	Hs.351906	ZNF506	−1.04186	−1.07409

Shown are the probeset identification code (PSID), the UniGene identification code, the gene symbol and the RMA-normalized fold changes from the whole-organ and LCM analyses

For the whole-organ analysis, RNA was isolated from entire tumors, or from whole LNs containing similar amounts of cancer cells within them. For LCM, RNA was isolated from 2,000 pure cancer cells of tumors and LN metastases (Fig. 1). To compare these sets we chose an approach that is commonly used to study large numbers of gene expression changes; namely, global gene expression profiling with Affymetrix gene chips. The chips used are designed to theoretically hybridize only with human RNA, and therefore both the whole-organ and LCM approaches should inform us only of the gene expression changes that occur in the human cancer cells within the mouse host sites. It was therefore surprising to find greater 'fold changes' in LN-specific genes assessed by LCM (Fig. 2a vs. Fig. 2b).

Since the gene chips used for the two methods interrogated the same transcripts, with all but 62 of the 61,358 X3P probesets having a matching U133+2 chip probeset, it was surprising that very few genes changed similarly between the two analyses (Fig. 3). Furthermore, of the 68 transcripts that were significantly different in LNs by both analyses, 38 were regulated in the opposite direction, being increased in the metastases by one analysis, and decreased by the other (Fig. 3a). These results suggest that the Affymetrix chips are binding not only human RNA but also mouse RNA. This aberrant hybridization may be

responsible not only for the gene differences reported by the two methods but also for the lack of overlap between the functional pathways identified.

No other reports have determined how sample collection methods influence LN metastasis gene signatures. However, one study [15] compared 28 breast tumors, 17 ER positive versus 11 ER negative, and identified genes differently expressed between these two cancer types using both LCM and bulk-tumor gene expression profiling. Interestingly, of all the genes found to be significantly different between ER positive and ER negative tumors, less than one-third were common to both analyses. These findings are interesting because the same human tumors were used for comparison, yet the ER signature changes were dependent on the type of analysis conducted.

We suggest two possible explanations for the differences between our whole organ and LCM-generated data. (1) It is possible that multiple unique transcripts are altered by the amplification procedure required for LCM. However, a previous study showed that amplification from the 3′ end of transcripts does not have a major impact on overall gene profiles with Affymetrix GeneChips because the probe sets on the arrays are designed using 3′ end sequences [16]. Additionally, another report found no significant differences in the expression intensity of 21 housekeeping genes from matched LCM and bulk-tumor gene expression data [15]. (2) An alternative hypothesis posits that Affymetrix chips can bind not only human RNA, but also mouse RNA, thus altering the chip readout from whole organ analyses. Naef et al. [17] recently tested this idea and found that indeed, mouse RNA hybridized to the "human-specific" gene chips. Interestingly, we found that on average 16.4% more probesets were present on whole-organ samples compared to LCM samples, suggesting that in xenografts, mouse RNA was contaminating the whole-organ analysis. The studies by Naef et al. suggest not only the possibility of cross-species contamination, but the possible skewing of data due to intraspecies contamination of tumor cells by normal epithelial, stromal, vascular, and immune tissue elements within an organ. Thus it may be critical to use LCM to determine how each tissue component of an organ contributes to the overall gene signature. Based on this, we suspect that our LCM data represent a more accurate gene expression comparison between tumors and their matched LN metastases.

These studies nevertheless identified 30 transcripts that were increased or decreased in LN metastases by both analyses (Table 1). These genes may represent the best targets for further studies to identify the mechanisms that contribute to the spread or growth of breast cancer cells into and within LNs. Prothymosin alpha (PTMA) was increased in the LN metastases and has previously been shown to increase proliferation rates of breast cancer cells [18]. This finding is interesting in view of our previous findings of increased proliferation rates in LN metastases [11]. Tumor necrosis factor receptor superfamily member 1A (TNFRSF1A) was also increased in the LN metastases. Its expression has previously been shown to decrease apoptosis in MCF-7 cells treated with human TNF alpha protein [19]. Ribonucleotide reductase M2 polypeptide (RRM2) and lymphotoxin beta receptor (LTBR) were both increased in the LN metastases, and both increase cancer cell survival [20, 21]. Interestingly, RRM2 is targeted by gemcitabine and hydroxyurea in lung and skin cancers, respectively [22]. A transcript whose expression was decreased in LN metastases and has been studied for its effects on cancer progression is caveolin-1 (CAV1). This scaffolding protein is the main component of the caveolae in plasma membranes of most cell types, and its expression inhibits proliferation in human breast cancer cells [23]. Its decreased expression may therefore play a role in the increased cell proliferation seen in LN metastases [11, 24].

In summary, this report evaluated whole-organ versus LCM for gene expression profiling, in order to identify therapeutic targets that may reduce breast cancer spread to and growth in LNs. However, when comparing these two experimental approaches, we found almost no overlap among the transcripts and functional pathways identified. The 30 transcripts that were common to both analyses may be the most promising for future therapeutic targeting. However, our data clearly demonstrate that the methods used to prepare tumors for gene expression profiling can markedly skew the results obtained.

References

1. van de Rijn M, Perou CM, Tibshirani R et al (2002) Expression of cytokeratins 17 and 5 identifies a group of breast carcinomas with poor clinical outcome. Am J Pathol 161(6):1991–1996
2. Zajchowski DA, Bartholdi MF, Gong Y et al (2001) Identification of gene expression profiles that predict the aggressive behavior of breast cancer cells. Cancer Res 61(13):5168–5178
3. Livasy CA, Perou CM, Karaca G et al (2007) Identification of a basal-like subtype of breast ductal carcinoma in situ. Hum Pathol 38(2):197–204
4. Chang HY, Nuyten DS, Sneddon JB et al (2005) Robustness, scalability, and integration of a wound-response gene expression signature in predicting breast cancer survival. Proc Natl Acad Sci USA 102(10):3738–3743
5. Chang HY, Sneddon JB, Alizadeh AA et al (2004) Gene expression signature of fibroblast serum response predicts human

cancer progression: similarities between tumors and wounds. PLoS Biol 2(2):E7

6. Rouzier R, Perou CM, Symmans WF et al (2005) Breast cancer molecular subtypes respond differently to preoperative chemotherapy. Clin Cancer Res 11(16):5678–5685

7. Weigelt B, Hu Z, He X et al (2005) Molecular portraits and 70-gene prognosis signature are preserved throughout the metastatic process of breast cancer. Cancer Res 65(20):9155–9158

8. Perou CM, Sorlie T, Eisen MB et al (2000) Molecular portraits of human breast tumours. Nature 406(6797):747–752

9. Shipitsin M, Campbell LL, Argani P et al (2007) Molecular definition of breast tumor heterogeneity. Cancer Cell 11(3):259–273

10. Fan C, Oh DS, Wessels L et al (2006) Concordance among gene-expression-based predictors for breast cancer. N Engl J Med 355(6):560–569

11. Harrell JC, Dye WW, Allred DC et al (2006) Estrogen receptor positive breast cancer metastasis: altered hormonal sensitivity and tumor aggressiveness in lymphatic vessels and lymph nodes. Cancer Res 66(18):9308–9315

12. Sartorius CA, Shen T, Horwitz KB (2003) Progesterone receptors A and B differentially affect the growth of estrogen-dependent human breast tumor xenografts. Breast Cancer Res Treat 79(3):287–299

13. Weigelt B, Wessels LF, Bosma AJ et al (2005) No common denominator for breast cancer lymph node metastasis. Br J Cancer 93(8):924–932

14. Montel V, Mose ES, Tarin D (2006) Tumor-stromal interactions reciprocally modulate gene expression patterns during carcinogenesis, metastasis. Int J Cancer 119(2):251–263

15. Yang F, Foekens JA, Yu J et al (2006) Laser microdissection and microarray analysis of breast tumors reveal ER-alpha related genes and pathways. Oncogene 25(9):1413–1419

16. Luzzi V, Mahadevappa M, Raja R, Warrington JA, Watson MA (2003) Accurate and reproducible gene expression profiles from laser capture microdissection, transcript amplification, and high density oligonucleotide microarray analysis. J Mol Diagn 5(1):9–14

17. Naef F, Huelsken J (2005) Cell-type-specific transcriptomics in chimeric models using transcriptome-based masks. Nucleic Acids Res 33(13):e111

18. Bianco NR, Montano MM (2002) Regulation of prothymosin alpha by estrogen receptor alpha: molecular mechanisms and relevance in estrogen-mediated breast cell growth. Oncogene 21(34):5233–5244

19. Pan G, Ni J, Wei YF, Yu G, Gentz R, Dixit VM (1997) An antagonist decoy receptor and a death domain-containing receptor for TRAIL. Science 277(5327):815–818

20. Force WR, Cheung TC, Ware CF (1997) Dominant negative mutants of TRAF3 reveal an important role for the coiled coil domains in cell death signaling by the lymphotoxin-beta receptor. J Biol Chem 272(49):30835–30840

21. Lin ZP, Belcourt MF, Cory JG, Sartorelli AC (2004) Stable suppression of the R2 subunit of ribonucleotide reductase by R2-targeted short interference RNA sensitizes p53(-/-) HCT-116 colon cancer cells to DNA-damaging agents and ribonucleotide reductase inhibitors. J Biol Chem 279(26):27030–27038

22. Barrons R (2004) Evaluation of personal digital assistant software for drug interactions. Am J Health Syst Pharm 61(4):380–385

23. Fiucci G, Ravid D, Reich R, Liscovitch M (2002) Caveolin-1 inhibits anchorage-independent growth, anoikis and invasiveness in MCF-7 human breast cancer cells. Oncogene 21(15):2365–2375

24. Hasebe T, Konishi M, Iwasaki M et al (2005) Histological characteristics of tumor cells and stromal cells in vessels and lymph nodes are important prognostic parameters of extrahepatic bile duct carcinoma: a prospective study. Hum Pathol 36(6):655–664